From Large Spin Hall Metal to Topological Chern Insulator: Materials Discovery through First-Principles Calculations

Guang-Yu Guo (郭光宇) [1,2]

[1]Department of Physics, National Taiwan University

[2]Physics Division, National Center for Theoretical Sciences

(NCTS 20th Anniversary Symposium: Frontiers in Physics,
NTHU Campus, Hsinchu, August 3, 2017)

Conventional superconductivity at 203 kelvin at high pressures in the sulfur hydride system [Nature 525 (2015) 73]

A. P. Drozdov[1]*, M. I. Eremets[1]*, I. A. Troyan[1], V. Ksenofontov[2] & S. I. Shylin[2]

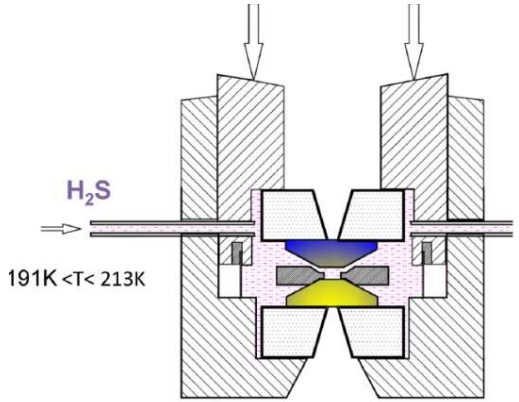

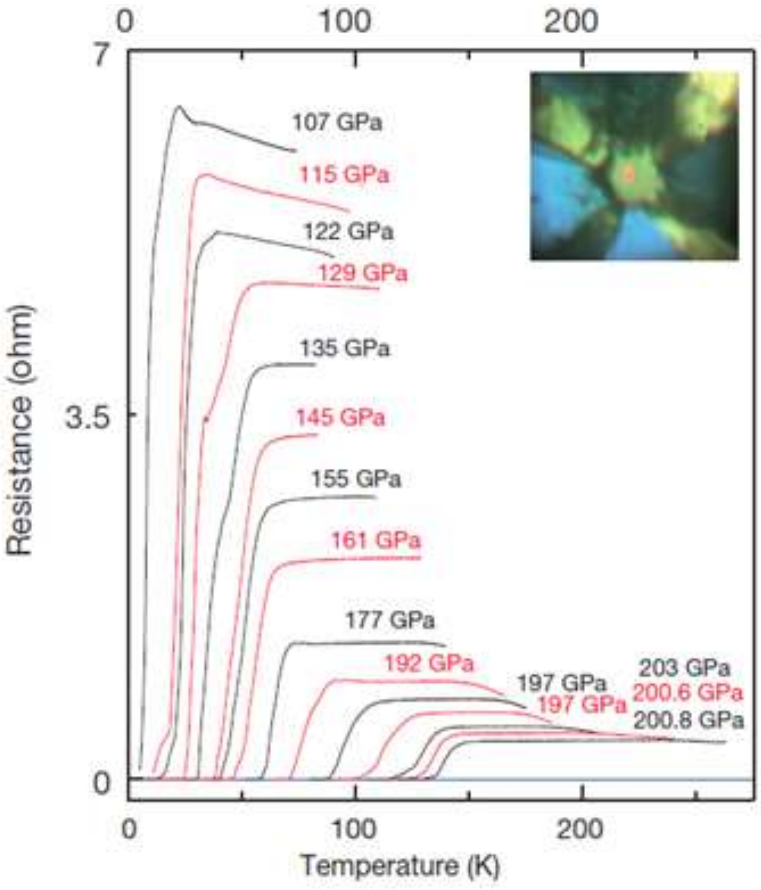

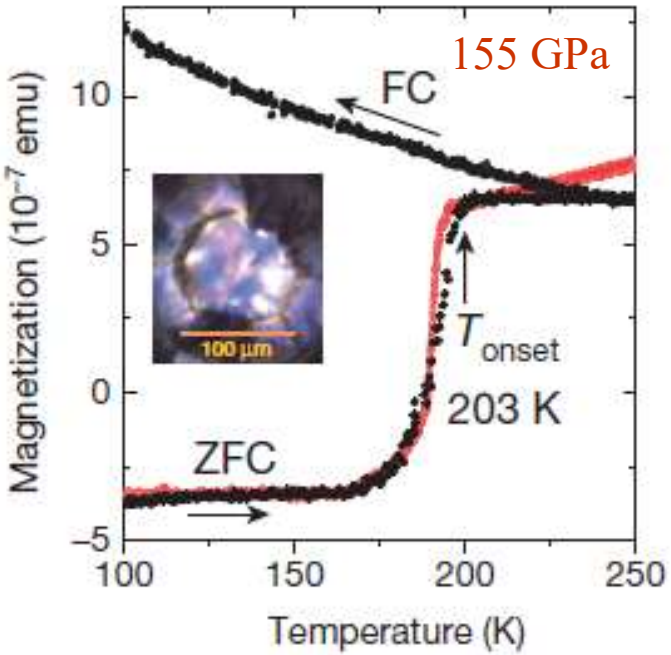

Cu oxides: Record T_C
133 K at ambient pressure
164 K at high pressure

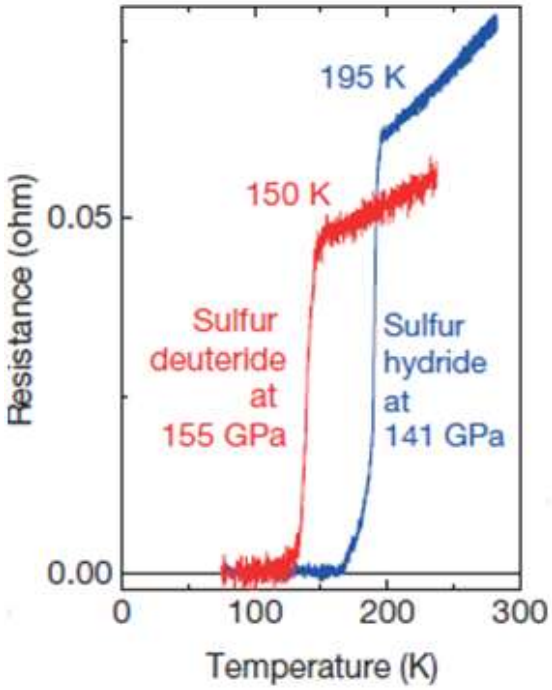

"We selected H_2S, because it is relatively easy to handle and is predicted to transform to a metal and a superconductor at a low pressure $P \approx 100$ GPa with a high $T_C = 80$ K [14] "

[Li, Hao, Liu, Li, Ma, JCP 140 (2014) 174712]

Prediction of mellalization and superconductivity of dense hydrogen sulfide

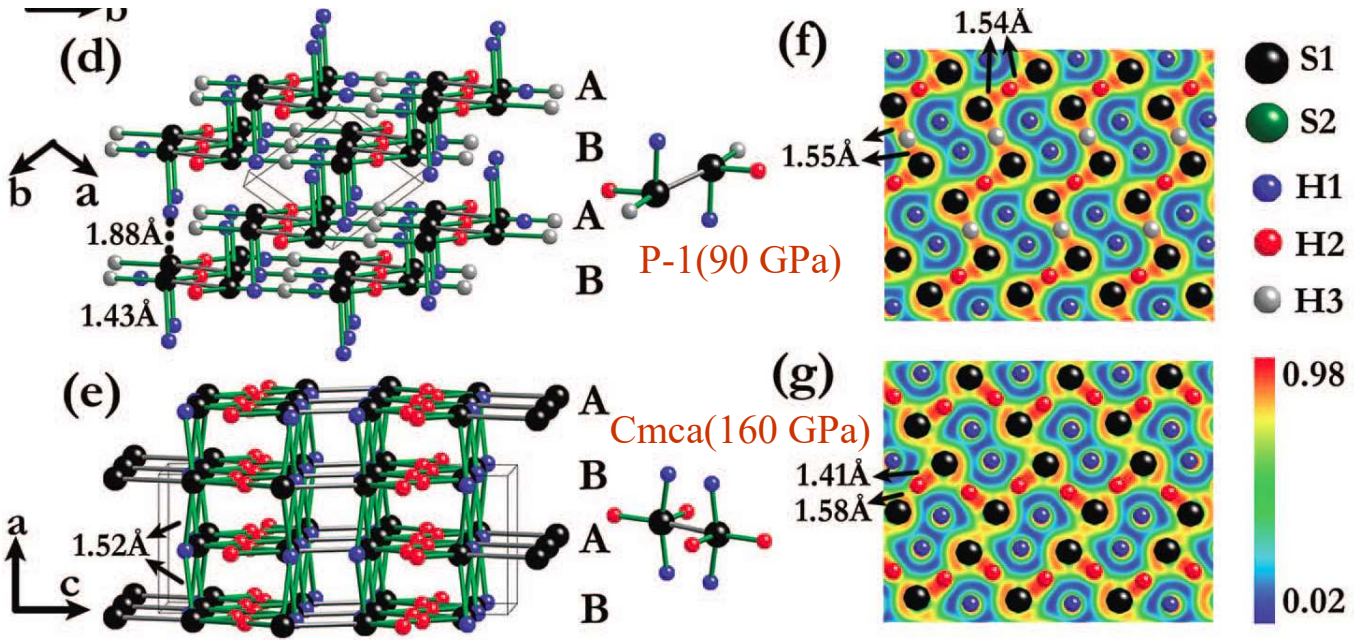

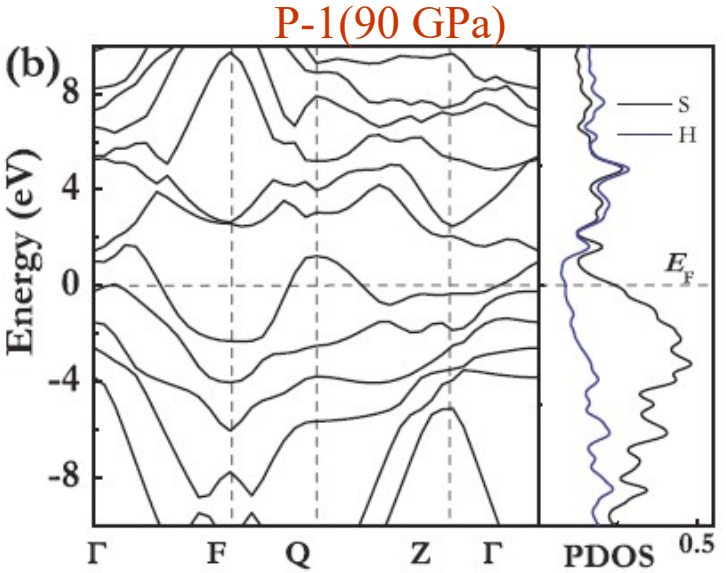

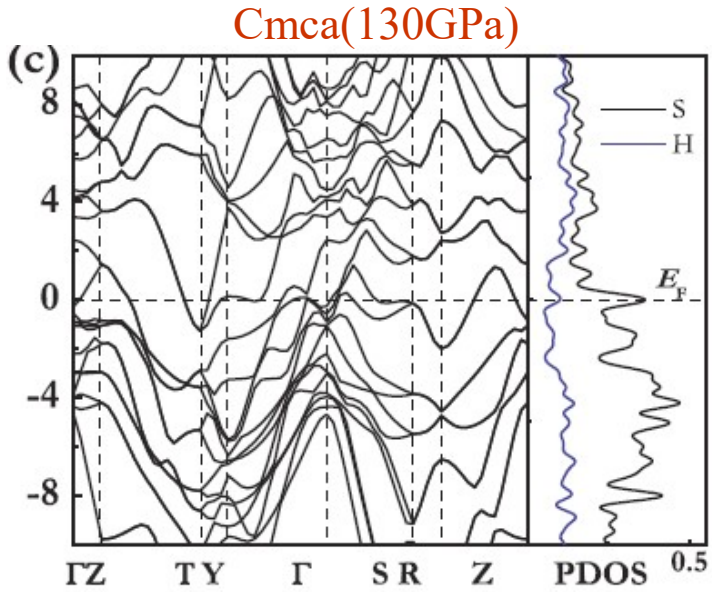

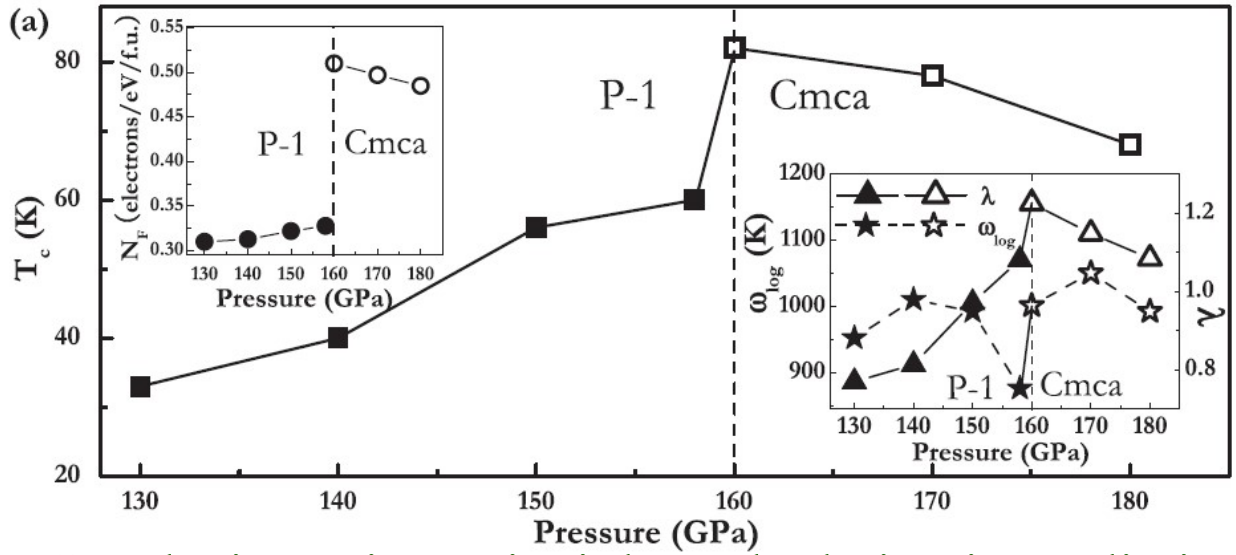

Conclusion: First-principles calculation is predictive and thus is a powerful tool in search for new materials such as high T_C superconductors.

Plan of this Talk

I. First-principles calculations in materials research

1. First-principles calculations
2. Significances of first-principles calculations

II. Spin Hall effect in solids

1. Concepts, observations and applications
2. Berry phase formalism for calculation of intrinsic Hall effects
3. Large intrinsic spin Hall effect in platinum metal

III. Multi-orbital Kondo effect in Fe-doped gold

1. Giant spin Hall effect in FePt/Au nanodevices
2. Multi-orbital Kondo effect

IV. Quantum topological Hall effect in chiral antiferromagnets

1. Quantum anomalous Hall effect
2. Quantum topological Hall effect in layered oxide K_xRhO_2

V. Conclusions

I. First-principles calculation in materials research

1. First-principles calculation

By first-principles (*ab initio*), we meant empirical parameter-free calculations by solving the Schrödinger equ. that describes the motion of electrons in the Coulomb potentials of nuclei and of each other; i.e., calculations in which the only input is the atomic numbers of the atoms and the macroscopic constraints (pressure, temperature, etc).

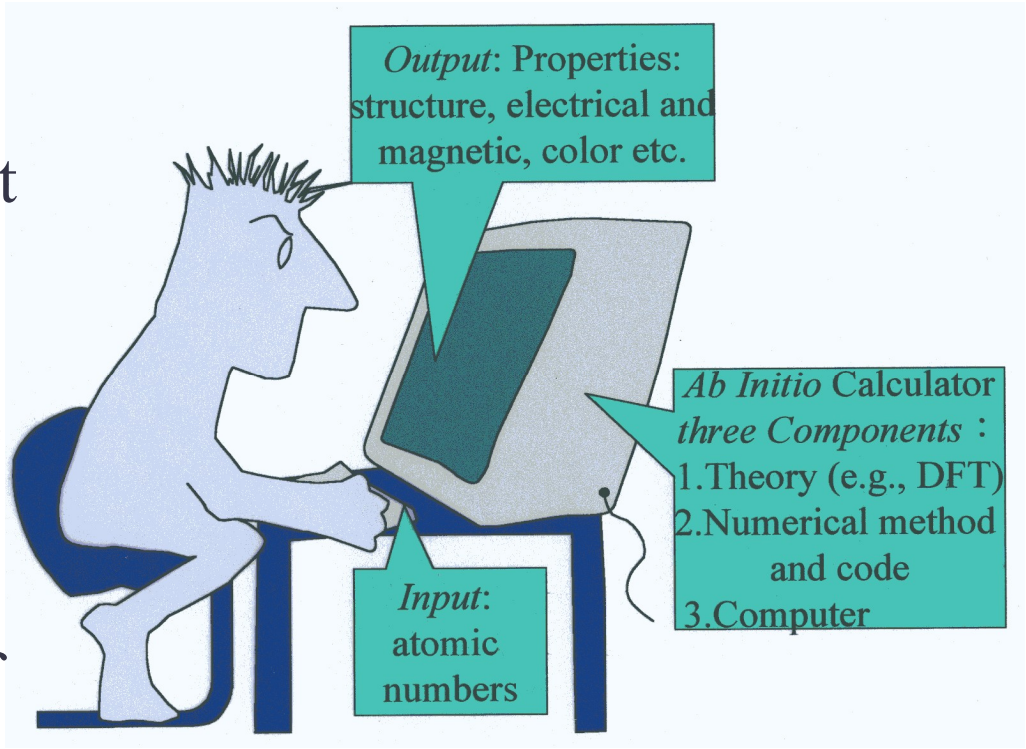

Cartoon of first-principles (*ab initio*) calculation

2. Significances of first-principles calculations

Today, due to advanced quantum theory, fast computers and efficient algorithms, first-principles calculations have become crucial to understand the intricate phenomena in condensed mater systems, to search for and even design new materials with desired properties.

Understanding intriguing complex phenomena in solids

1) Si (111)-(7×7) surface reconstruction

VOLUME 68, NUMBER 9 PHYSICAL REVIEW LETTERS 68, 1355 2 MARCH 1992

Ab Initio Theory of the Si(111)-(7×7) Surface Reconstruction

Karl D. Brommer,[1] M. Needels,[2] B. E. Larson,[3] and J. D. Joannopoulos[1]

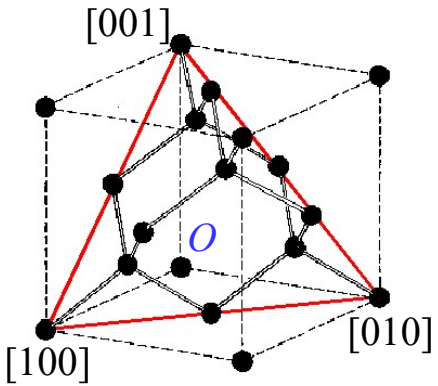

Bulk Si in diamond structure

Truncated Si(111)-(1×1) surface

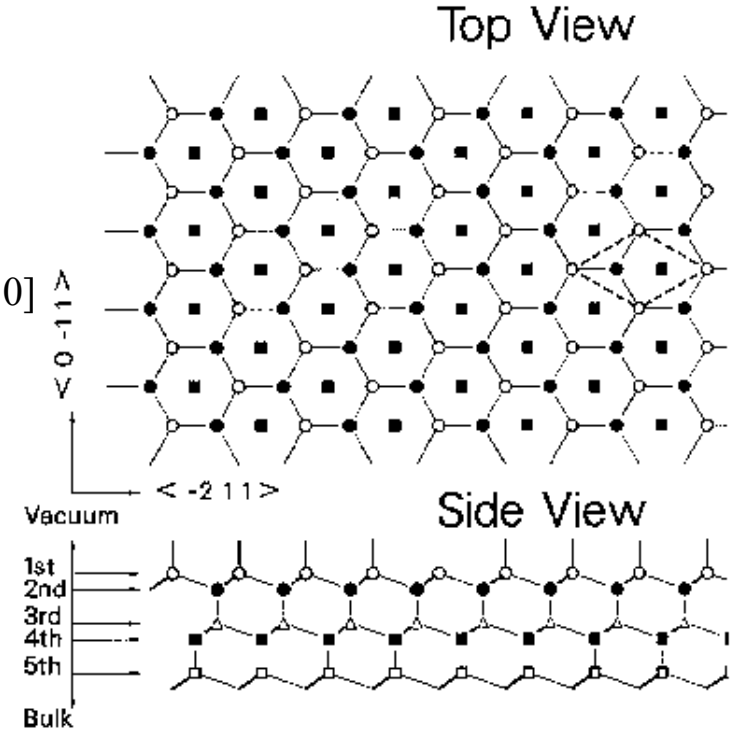

Reconstructed Si(111)-(7×7) surface

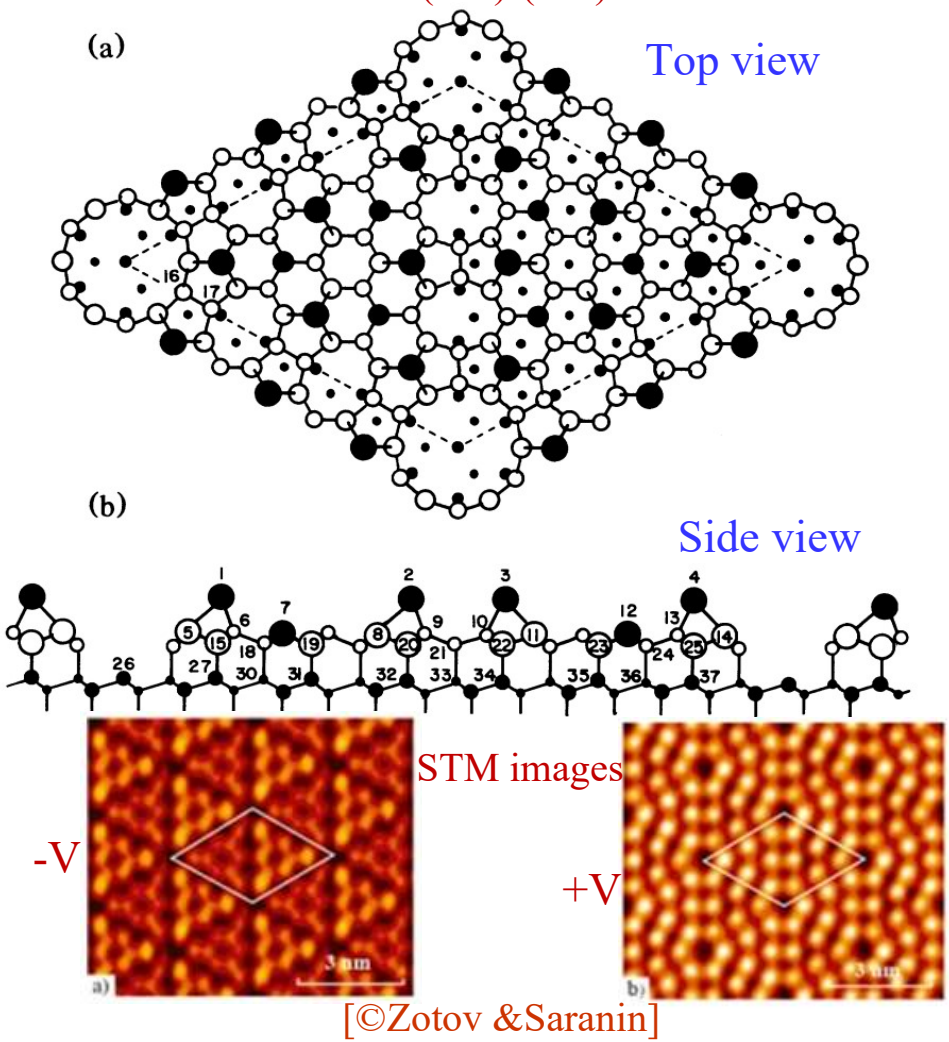

[©Zotov &Saranin]

Ab initio calculations determine (1) the energy differences among the different surface structures, (2) the atomic structure and (3) the STM images.

2) Charge-orbital ordering in magnetite (Fe_3O_4)

(a) Charge and orbital ordering in oxides

Charge ordering: Spatial localization of charge carriers on certain ionic sites.

Orbital ordering: Real space ordering of charge carriers on certain orbitals.

Charge and orbital ordering is intimately related to structural, magnetic and transport properties, e.g., colossal magnetoresistance or even high Tc superconductivity by dynamical charge-orbital fluctuation.

Charge-ordered stripe pairs

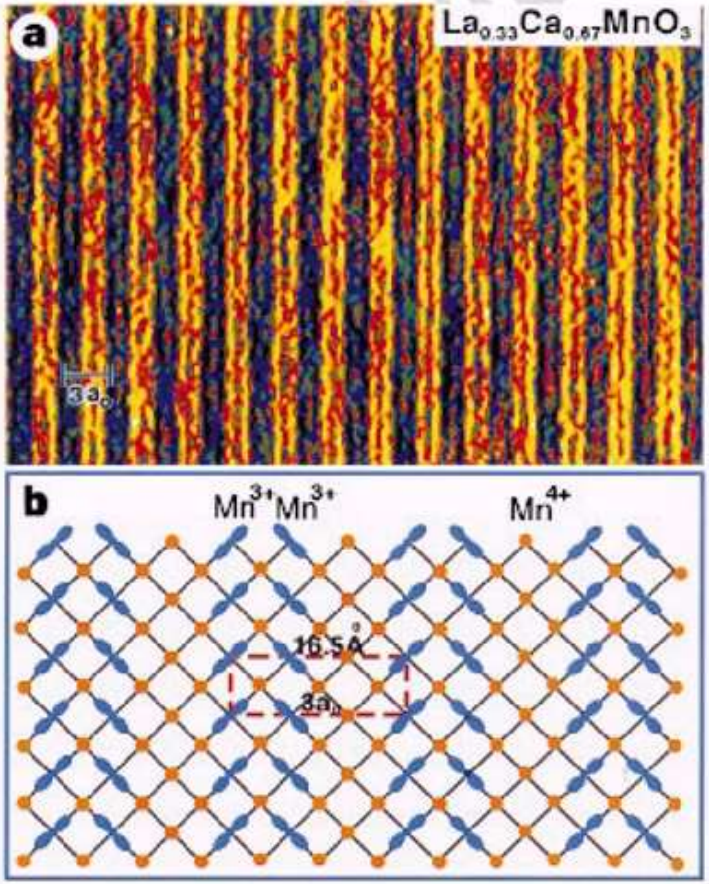

[Mori, Chen, Cheong, Nature 392 (1998) 473]

Orbital and spin orderings

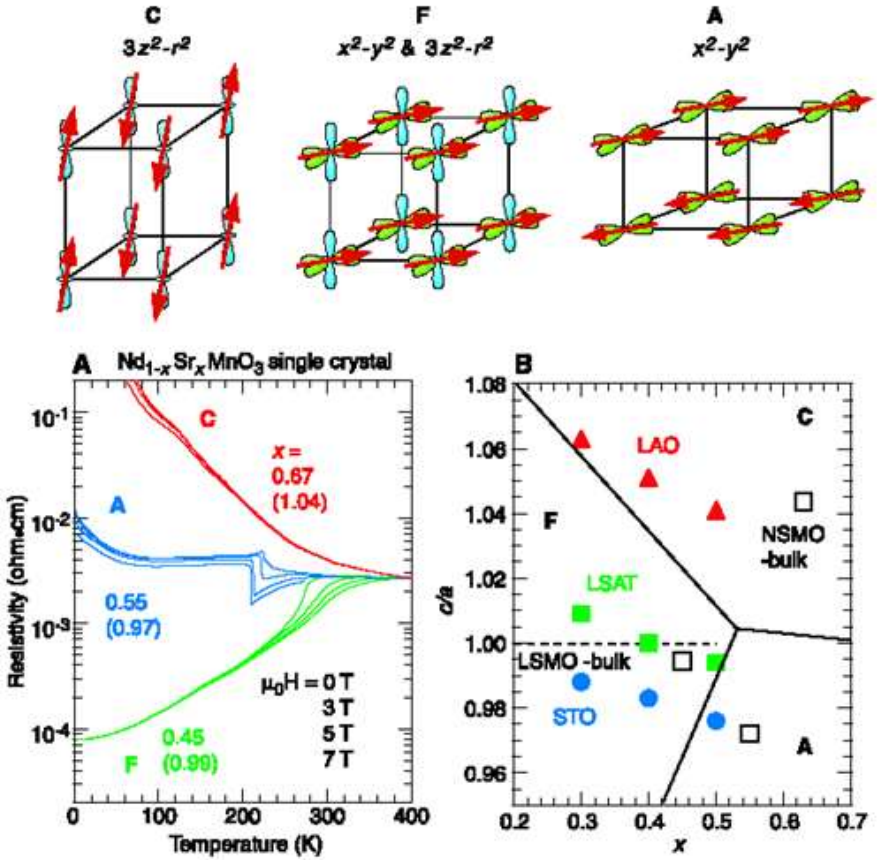

[Tokura, Nagaosa, Science 288 (2000) 462]

(b) Verwey transition in magneite (Fe_3O_4)

The classic charge ordering problem is however that of magnetite (1941).

The oldest magnet known to mankind, as magic stones (2500 yrs).

Metal-insulator (Verwey) transition

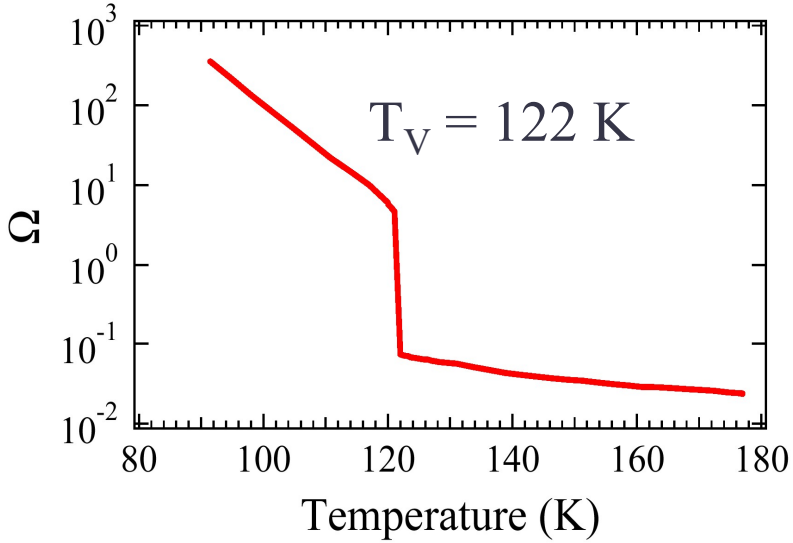

Ferrimagnetic

A-site ↓, B-site ↑, $T_C \sim 860K$

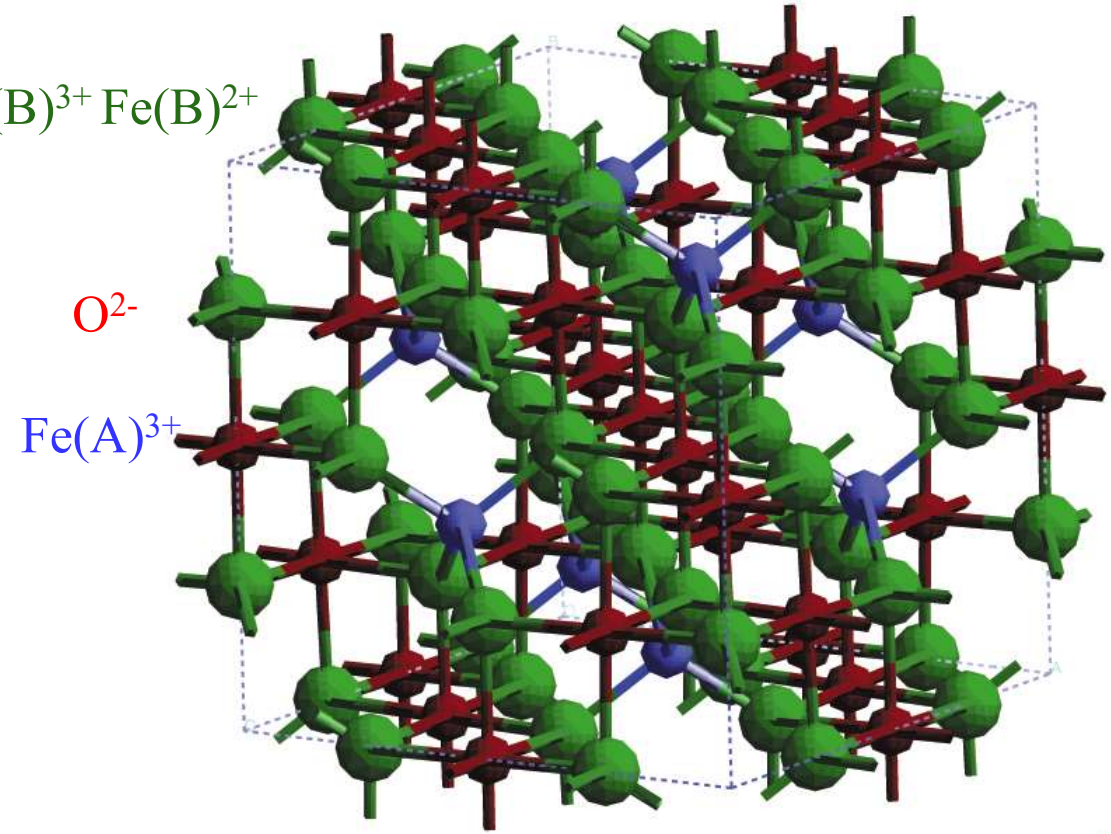

Inverted spinel structure above T_V

1/3: tetrahedral (A-site)) Fe^{3+}

2/3: octahedral (B-site) Fe^{3+}, Fe^{2+}

Verwey charge ordering model for M-I transition (1941):

The M-I transition is due to a charge ordering of the Fe^{2+} and Fe^{3+} states on the B sublattice, resulting in an orthorhombic structure.

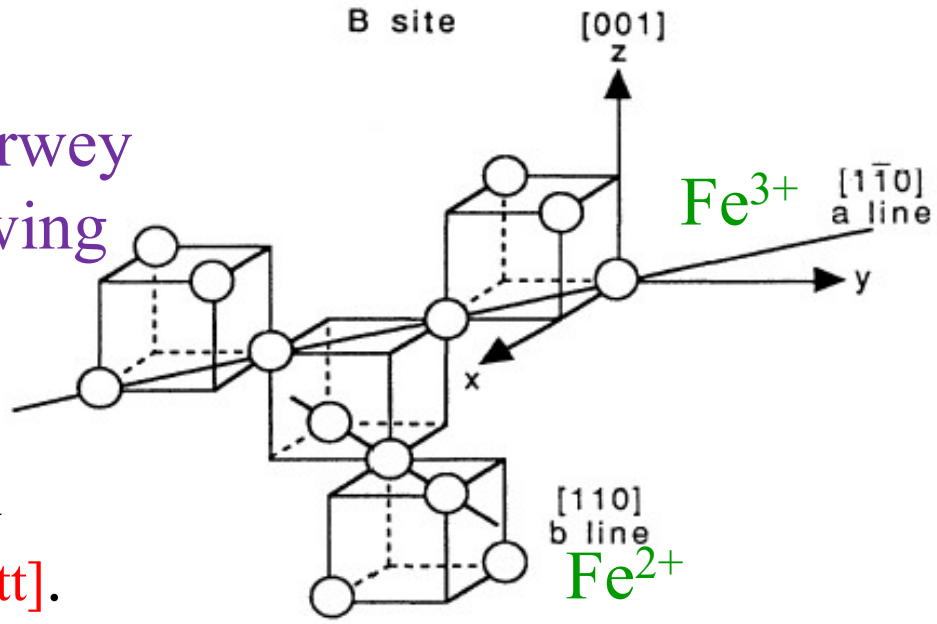

Simple Verwey model was later disproved [Walz, JPCM 2002] and mechanism of Verwey transition remains unresolved in the following 60 years despite intensive investigations

Many theoretical models were proposed, including Anderson criterion [Anderson] and Wigner glass-Wigner crystal transition [Mott].

In 1979, N.V. Mott called for an international workshop completely dedicated to the Verwey transition [Philos. Mag. B 42 (1980)].

A long review paper appears in JPCM 14 (2002) R285 (Walz) saying that many experimental aspects are clear now but the fundamental issues remain.

Yet, another review two years later also in JPCM 16 (2004) R145 saying "In this review, we will refute all the arguments advanced by that author."

(c) Discovery of charge-orbital ordering by first-principles calculations

VOLUME 93, NUMBER 15 PHYSICAL REVIEW LETTERS week ending 8 OCTOBER 2004

[PRL 93 (2004) 156403]

Charge-Orbital Ordering and Verwey Transition in Magnetite

Horng-Tay Jeng,[1,*] G. Y. Guo,[2,3,†] and D. J. Huang[3]

Calculated band structure

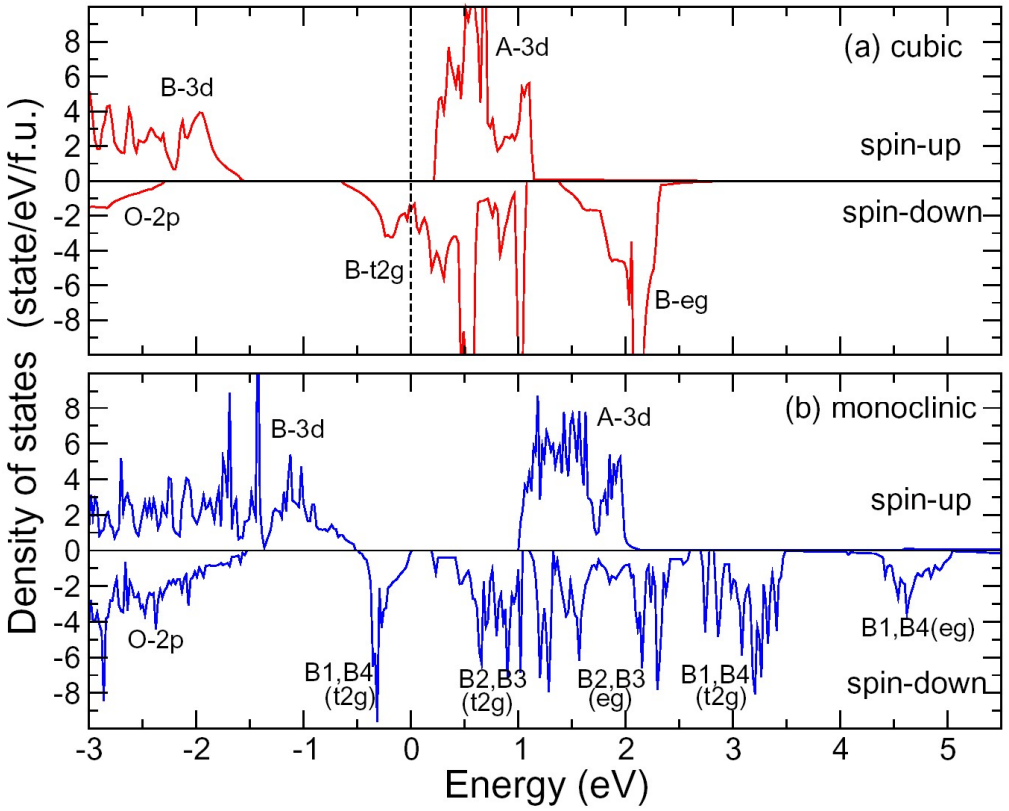

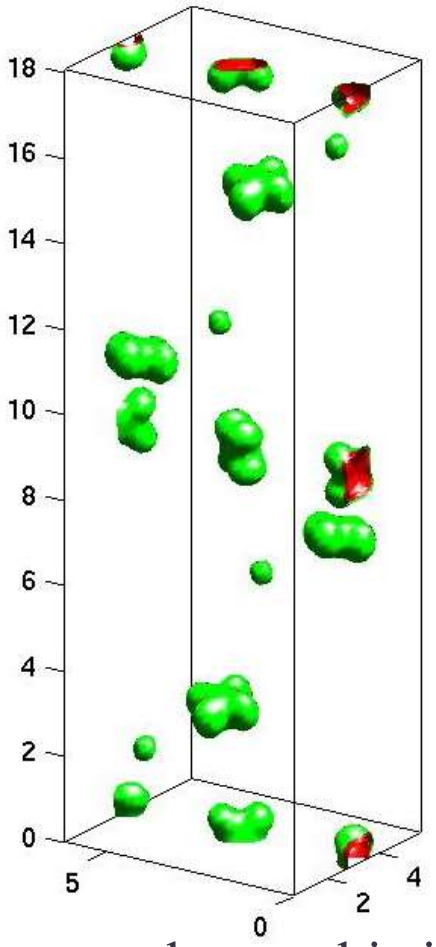

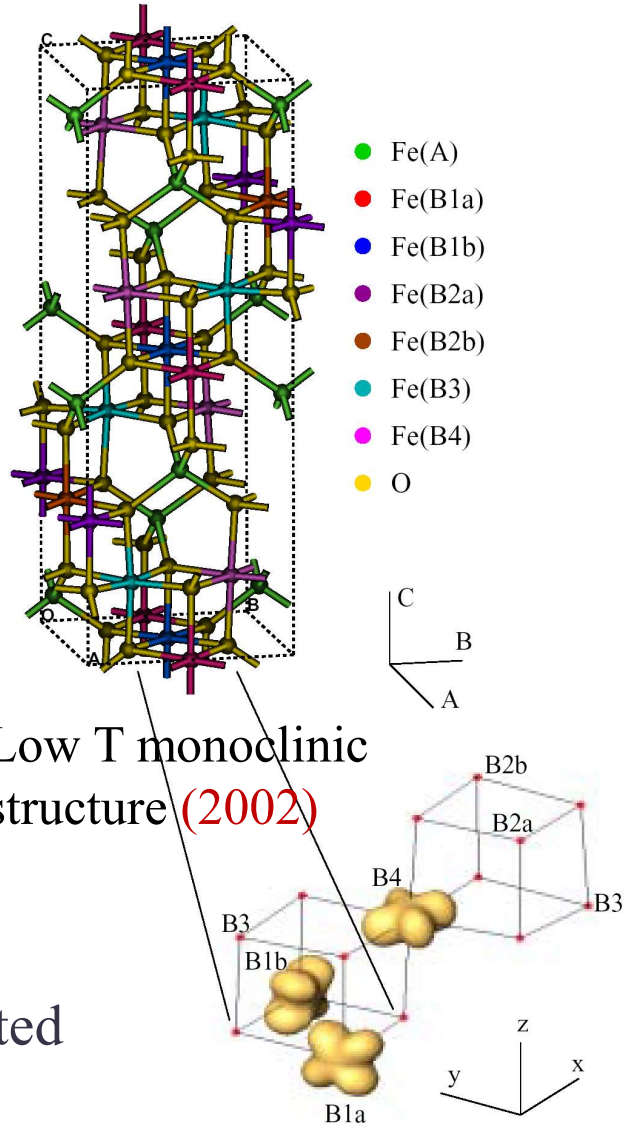

Low T monoclinic structure (2002)

Calculated charge distribution reveals a sophisticated Fe t_{2g}-orbital ordering on B-site sublattice.

(d) Confirmation by O K-edge resonant x-ray scattering experiments

[Huang, et al., Phys. Rev. Lett. 96, 096401 (2006)]

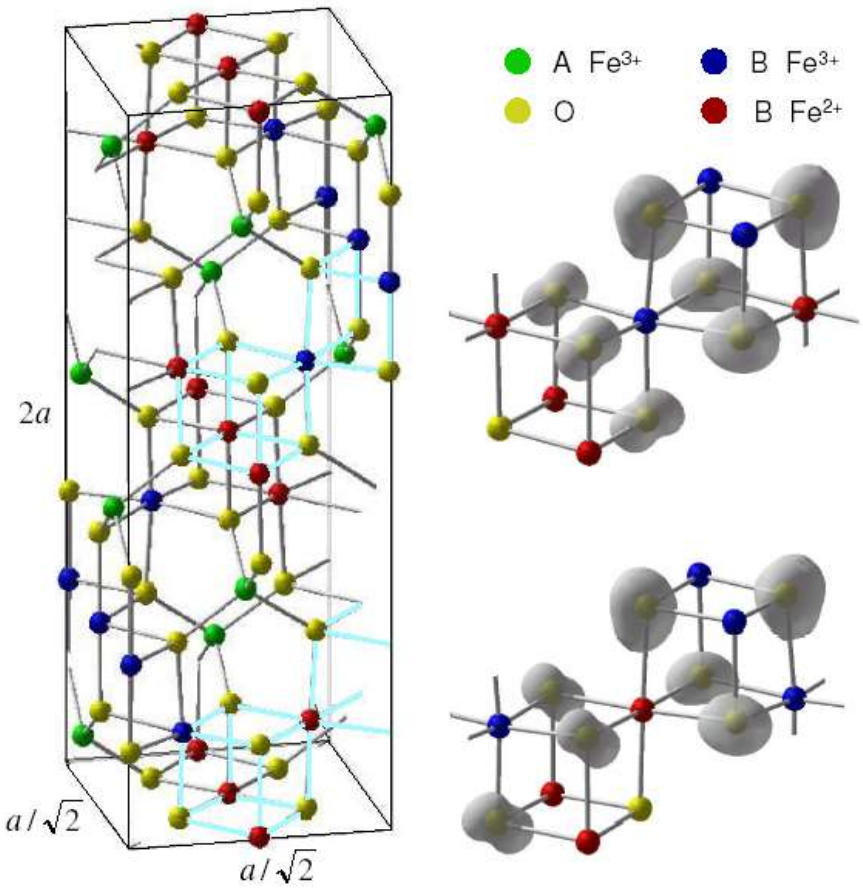

Unoccupied O 2p orbital ordering

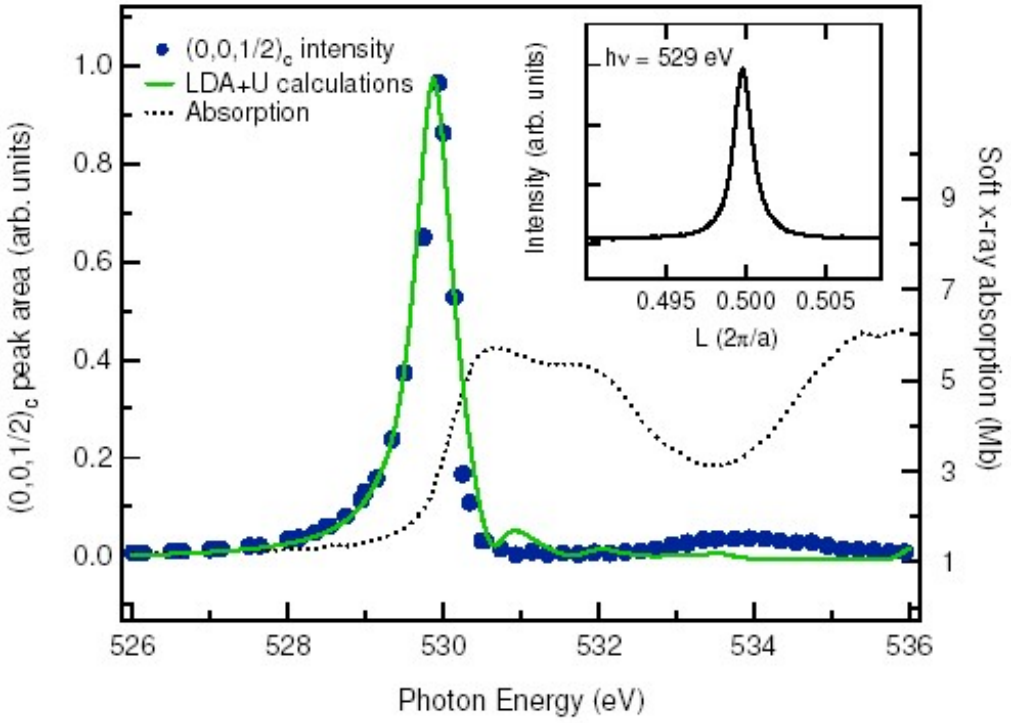

O K-edge X-ray absorption and resonant scattering spectra

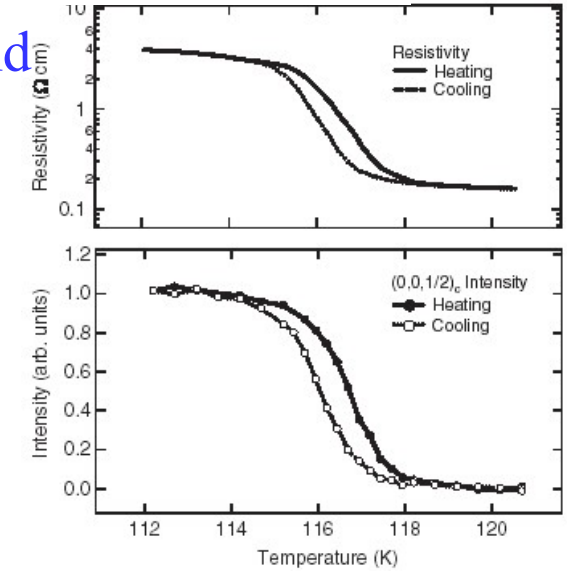

Thus, first-principles calculations help to solve this long standing (60 yrs) problem (classical charge ordering) in solid state physics.

II. Spin Hall effect in solids

1. Concepts, observations and applications

1) Ordinal Hall Effect [Hall 1879]

Lorentz force

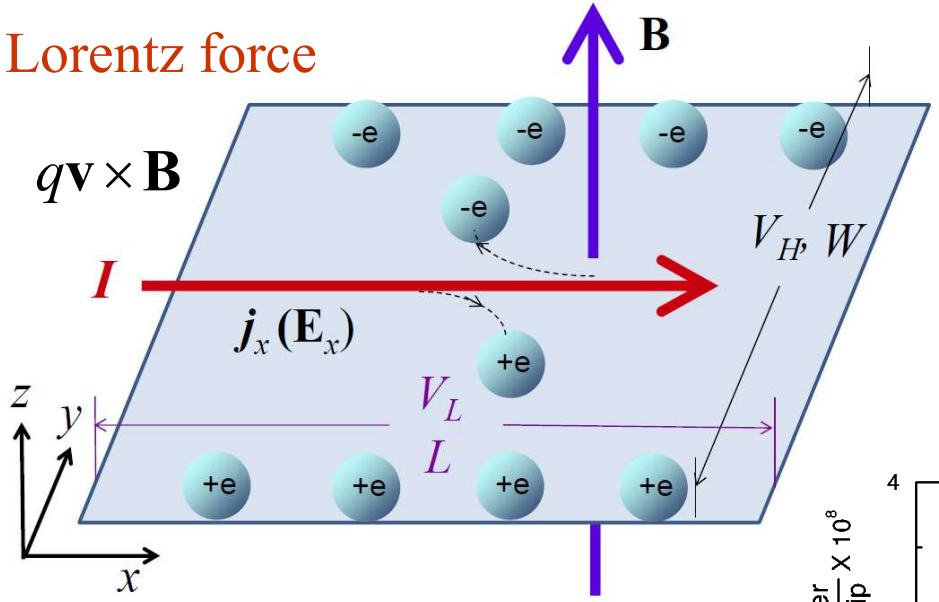

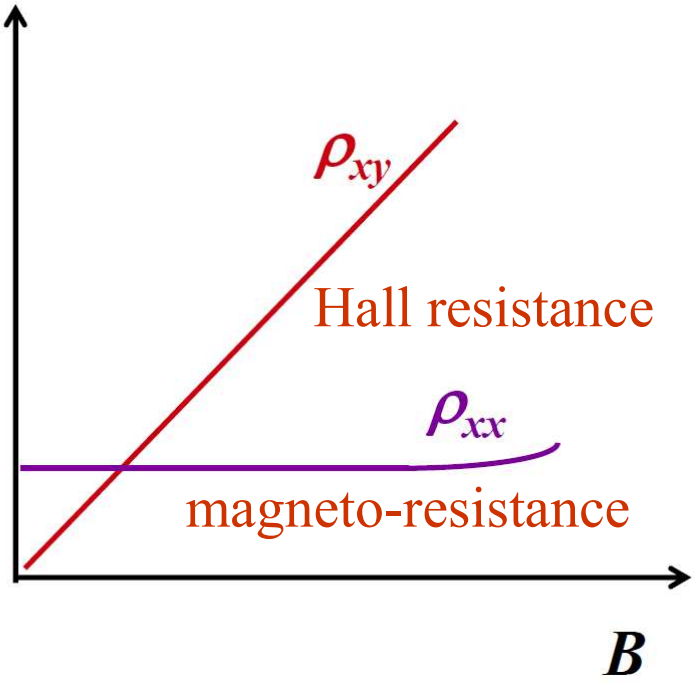

$$R_L = V_L / I = (E_x L)/(j_x W) = \rho_{xx}(L/W)$$

$$R_H = V_H / I = (E_y W)/(j_x W) = \rho_{xy} = (1/nq)B$$

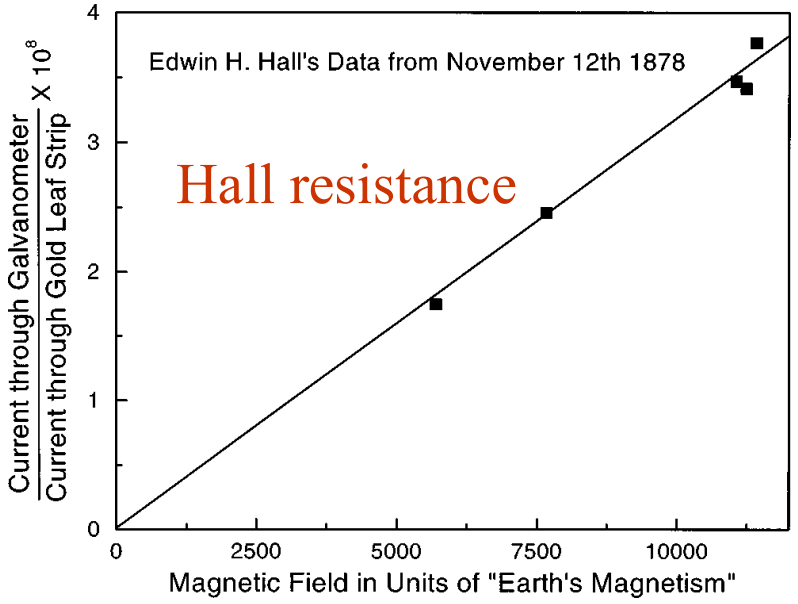

Edwin H. Hall (1855-1938)

OHE is a widely used characterization tool in material science lab.

2) Anomalous Hall Effect [Hall 1881]

(Hall effect with applied magnetic field)

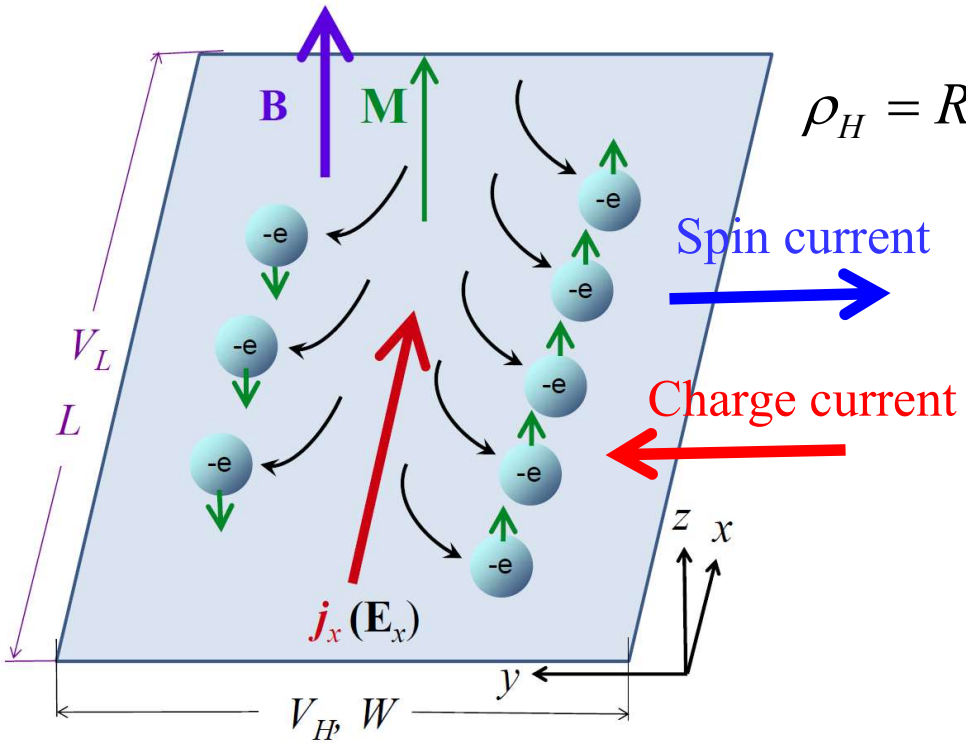

$$\rho_H = R_0 B + R_S M$$

Mn_5Ge_3 [Zeng et al. PRL 96 (2006) 2010]

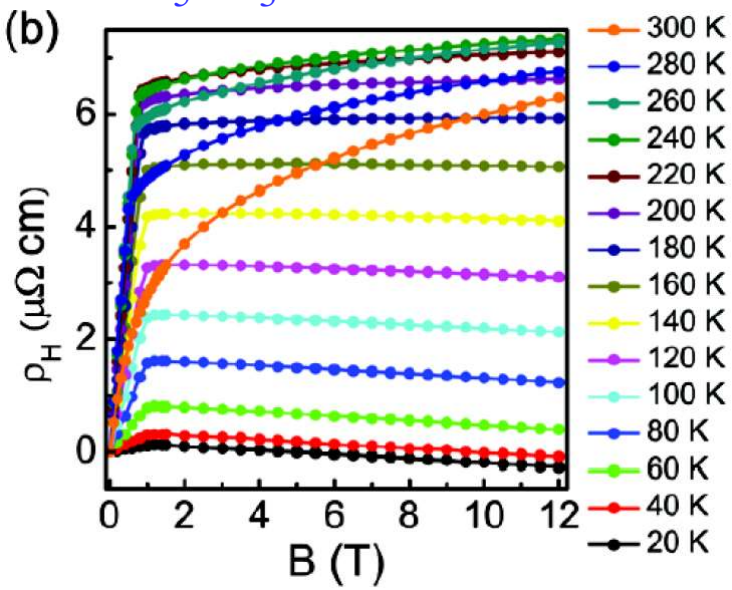

Relativistic spin-orbit coupling [Jackson's textbook]

$$\vec{B}' = -\gamma \frac{\vec{v}}{c} \times \vec{E} \approx -\frac{\vec{E} \times \vec{p}}{mc} = \frac{1}{mc} \nabla V(\mathbf{r}) \times \vec{p},$$

$$H_{SO} = -\vec{\mu} \cdot \vec{B}' = -\frac{1}{2m^2c^2} \vec{s} \cdot (\nabla V(\mathbf{r}) \times \vec{p})$$

$$H_{SO} = -\frac{1}{2m^2c^2} \vec{s} \cdot (\frac{dV}{dr} \frac{\vec{r}}{r} \times \vec{p}) \approx -\frac{Ze^2}{2m^2c^2r^3} (\vec{s} \cdot \vec{L})$$

(Mott or skew scattering)

3) Spin Hall Effect

[Dyakonov & Perel, JETP 1971]

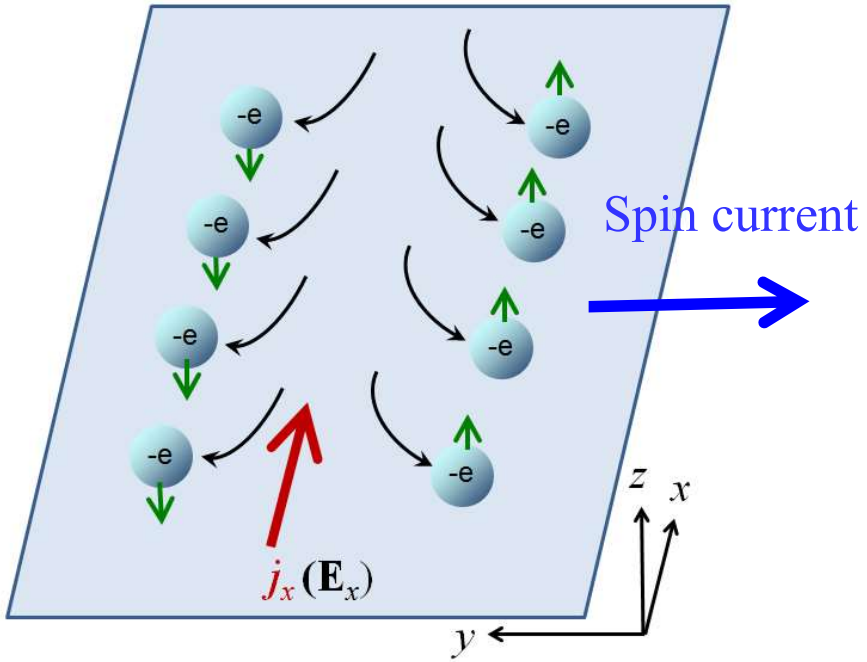

4) Intrinsic spin Hall effect

Dissipationless Quantum Spin Current at Room Temperature

Shuichi Murakami,[1*] Naoto Nagaosa,[1,2,3] Shou-Cheng Zhang[4]

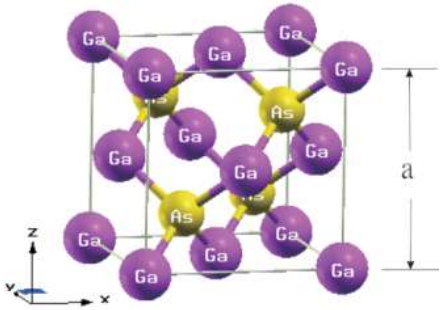

[Science 301, 1348 (2003)]

Luttinger model $$H_0 = \frac{\hbar^2}{2m}\left[(\gamma_1 + \frac{5}{2}\gamma_2)k^2 - 2\gamma_2(\vec{k}\cdot\vec{S})^2\right]$$

Dirac monopole $$F_{ij} \equiv i[D_i, D_j] = \epsilon_{ijk}\lambda\frac{k_k}{k^3}$$

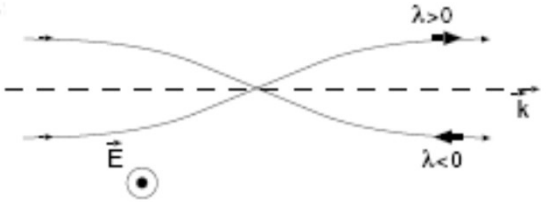

Equation of motion $$\left\langle \dot{X}_i \right\rangle = \frac{\hbar k_i}{m_\lambda} + F_{il}\left\langle \dot{k}_l \right\rangle$$

$$\left\langle \dot{k}_i \right\rangle = \frac{e}{\hbar}E_i \qquad e > 0 \ \text{(hole)}$$

Anomalous velocity $$\left\langle \dot{\vec{X}} \right\rangle = \frac{\hbar\vec{k}}{m_\lambda} - \frac{e\lambda}{\hbar k^3}\vec{k}\times\vec{E}$$

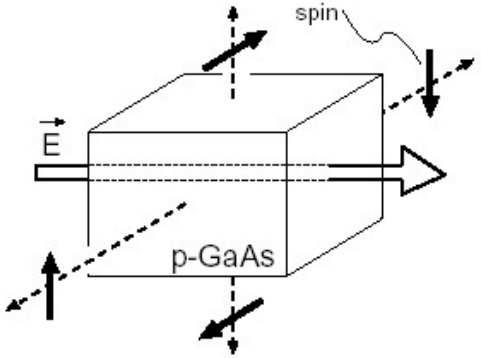

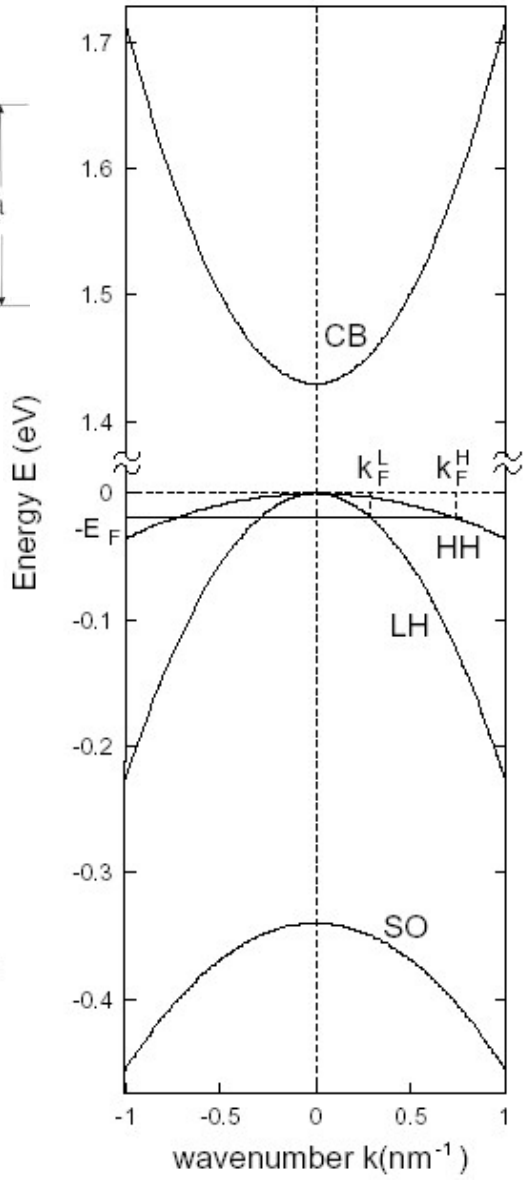

$$j_j^i = \sigma_s \varepsilon^{ijk} E_k$$

$$j_y^x = \frac{eE_z}{12\pi^2}(3k_F^{\mathrm{H}} - k_F^{\mathrm{L}}) = \frac{\hbar}{2e}\sigma_s E_z$$

$n_h = 10^{19}$ cm^{-3}, μ= 50 cm /V·s, σ= $e\mu n_h$ = 80 Ω^{-1}cm^{-1};
σ_s= 80 Ω^{-1}cm^{-1}

$n_h = 10^{16}$ cm^{-3}, μ= 50 cm /V·s, σ= $e\mu n_h$ = 0.6 Ω^{-1}cm^{-1};
σ_s= 7 Ω^{-1}cm^{-1}

5) Observations of spin Hall effect in semiconductors

First observation of SHE in n-type GaAs films

[Kato *et al.*, Science 306, 1910 (2004)]

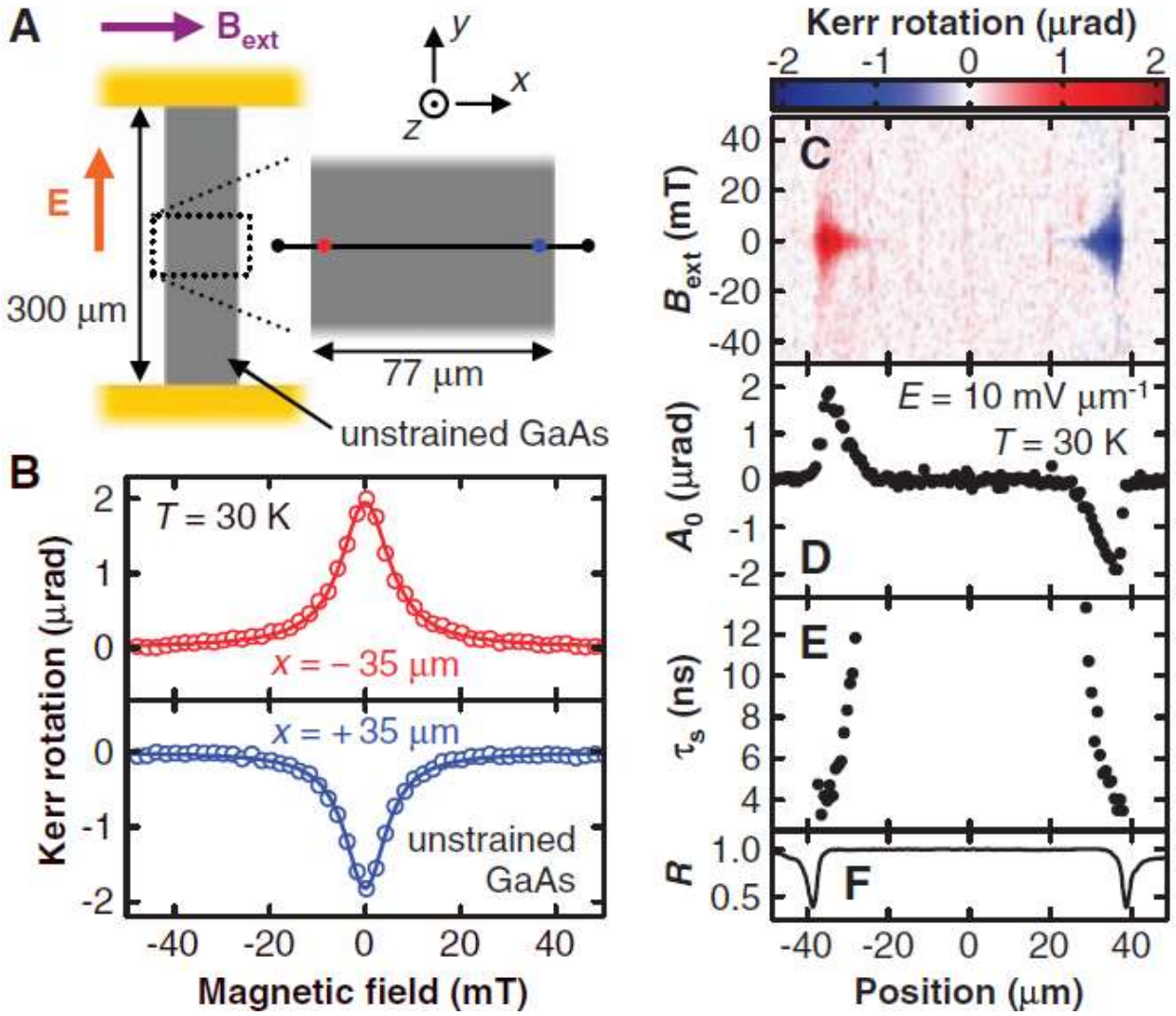

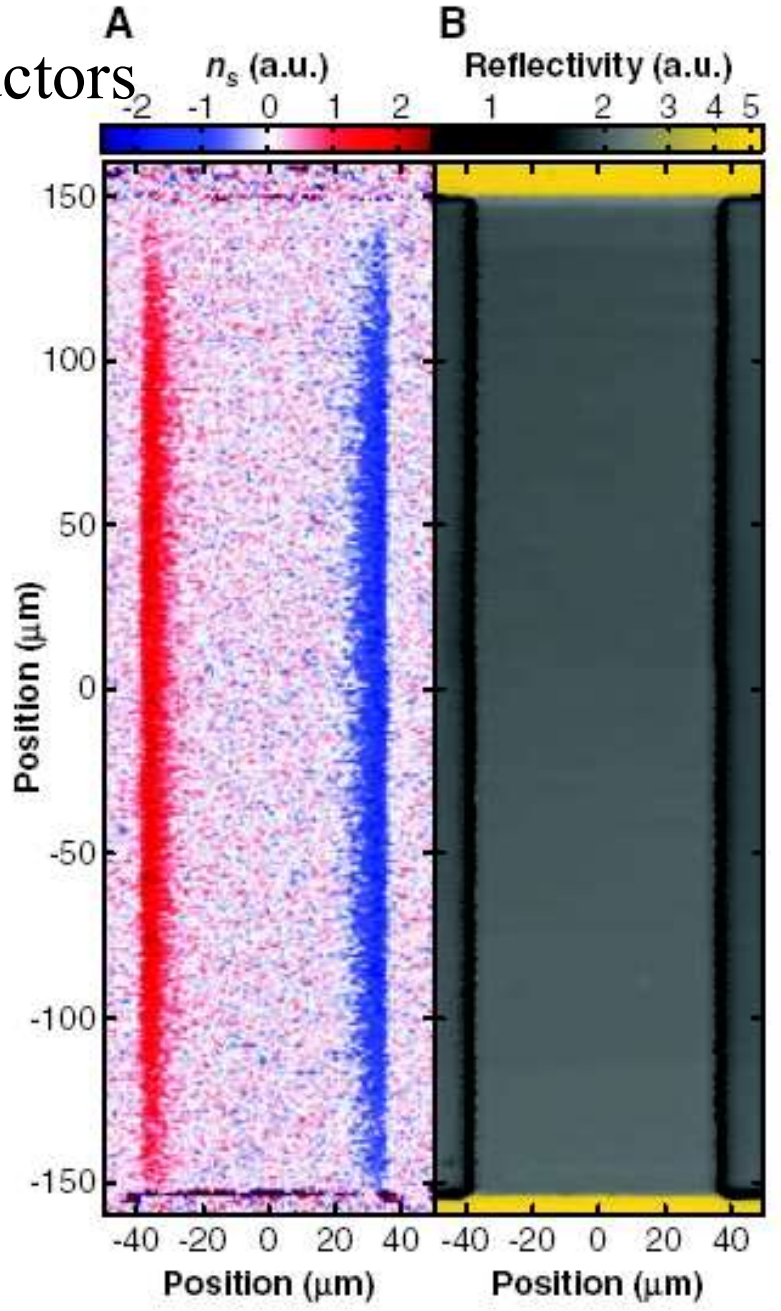

Fig. 2. (**A** and **B**) Two-dimensional images of spin density n_s and reflectivity R, respectively, for the unstrained GaAs sample measured at T = 30 K and E = 10 mV μm^{-1}.

6) Importance of spin Hall effect

Spintronics (spin electronics)

Three basic elements: Generation, detection, & manipulation of spin current.

Usual spin current generations: Ferromagnetic leads

Problems: magnets and/or magnetic fields needed, and difficult to integrate with semiconductor technologies.

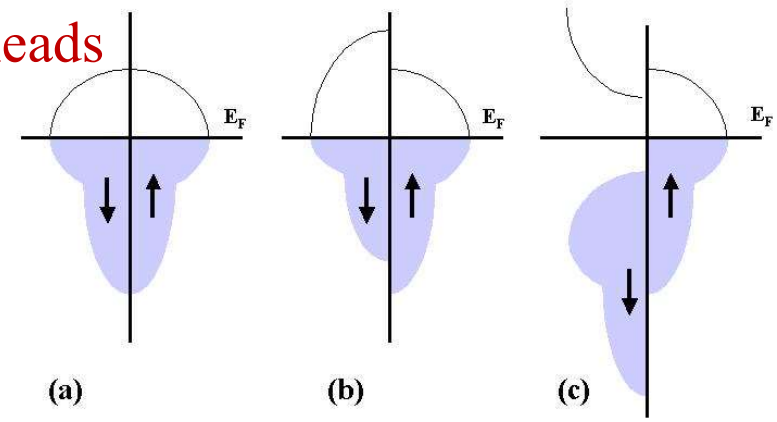

(a) non-magnetic metals, (b) ferromagnetic metals and (c) half-metallic metals.

(i) Spin Hall effect would allow us to generate pure spin current electrically in nonmagnetic microstructures without applied magnetic fields or magnetic materials, and make possible pure electric driven spintronics which could be readily integrated with conventional electronics.

(ii) Inverse spin Hall effect would enable us to detect spin current electrically, again without applied magnetic fields or magnetic materials.

2. Berry phase formalism for calculation of intrinsic Hall effects

1) Semiclassical dynamics of Bloch electrons

Old version [e.g., Aschroft, Mermin, 1976]

$$\dot{\mathbf{x}}_c = \frac{1}{\hbar}\frac{\partial \varepsilon_n(\mathbf{k})}{\partial \mathbf{k}},$$

$$\dot{\mathbf{k}} = -\frac{e}{\hbar}\mathbf{E} - \frac{e}{\hbar}\dot{\mathbf{x}}_c \times \mathbf{B} = \frac{e}{\hbar}\frac{\partial \varphi(\mathbf{r})}{\partial \mathbf{r}} - \frac{e}{\hbar}\dot{\mathbf{x}}_c \times \mathbf{B}.$$

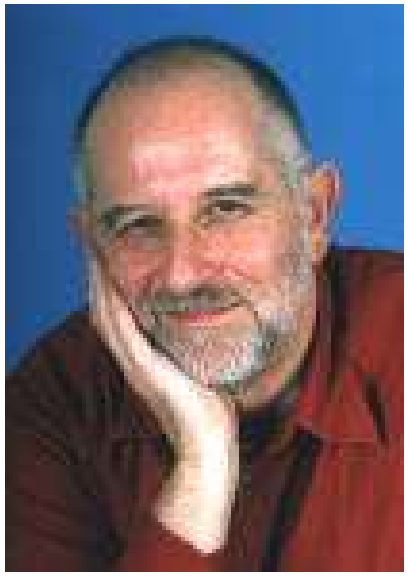

Michael Berry (1941-)

Berry phase correction

$$\dot{\mathbf{x}}_c = \frac{1}{\hbar}\frac{\partial \varepsilon_n(\mathbf{k})}{\partial \mathbf{k}} - \dot{\mathbf{k}} \times \boldsymbol{\Omega}_n(\mathbf{k}),$$

$$\dot{\mathbf{k}} = \frac{e}{\hbar}\frac{\partial \phi(\mathbf{r})}{\partial \mathbf{r}} - \frac{e}{\hbar}\dot{\mathbf{x}}_c \times \mathbf{B},$$

[Chang & Niu, PRL (1995), PRB (1996);
Xiao, Chang & Niu, RMP 82, 1959 (2010)]

$$\boldsymbol{\Omega}_n(\mathbf{k}) = -\mathrm{Im}\left\langle \frac{\partial u_{n\mathbf{k}}}{\partial \mathbf{k}} \right| \times \left| \frac{\partial u_{n\mathbf{k}}}{\partial \mathbf{k}} \right\rangle.$$ (Berry curvature)

2) Semiclassical transport theory

$$\mathbf{j} = \int d^3k(-e\dot{\mathbf{x}})g(\mathbf{r},\mathbf{k}), \qquad g(\mathbf{r},\mathbf{k}) = f(\mathbf{k}) + \delta f(\mathbf{r},\mathbf{k})$$

$$\dot{\mathbf{x}} = \frac{\partial \varepsilon_n(\mathbf{k})}{\hbar \partial \mathbf{k}} + \frac{e}{\hbar}\mathbf{E}\times\boldsymbol{\Omega}$$

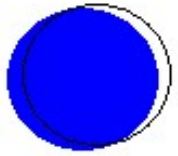

(ordinary conductance)

$$\mathbf{j} = -\frac{e^2}{\hbar}\mathbf{E}\times\int d^3\mathbf{k} f(\mathbf{k})\boldsymbol{\Omega} - \frac{e}{\hbar}\int d^3\mathbf{k}\delta f(\mathbf{k},\mathbf{r})\frac{\partial \varepsilon_n(\mathbf{k})}{\partial \mathbf{k}}$$

(Anomalous Hall conductance)

Anomalous Hall conductivity

$$\sigma_{xy} = -\frac{e^2}{\hbar}\int d^3\mathbf{k}\sum_n f(\varepsilon_n(\mathbf{k}))\Omega_n^z(\mathbf{k})$$

$$\Omega_n^z(\mathbf{k}) = -\sum_{n'\neq n}\frac{2\,\mathrm{Im}\langle \mathbf{k}n | v_x | \mathbf{k}n'\rangle\langle \mathbf{k}n' | v_y | \mathbf{k}n\rangle}{(\omega_{\mathbf{k}n'} - \omega_{\mathbf{k}n})^2}$$

3) *Ab initio* relativistic band structure methods

Calculations must be based on a relativistic band theory because all the intrinsic Hall effects are caused by spin-orbit coupling.

Relativistic linear muffin-tin orbital (LMTO) method.

[Ebert, PRB 1988; Guo & Ebert, PRB 51, 12633 (1995)]

Dirac Hamiltonian $H_D = c\boldsymbol{\alpha}\cdot\mathbf{p} + mc^2(\beta - I) + v(\mathbf{r})I$

[Guo, Yao, Niu, PRL 94, 226601 (2005)]

$$\sigma_{xy} = \frac{e}{\hbar}\int d^3\mathbf{k}\sum_n f(\varepsilon_n(\mathbf{k}))\Omega_n^z(\mathbf{k})$$

$$\Omega_n^z(\mathbf{k}) = -\sum_{n'\neq n}\frac{2\,\mathrm{Im}\left\langle \mathbf{k}n \mid j_x \mid \mathbf{k}n'\right\rangle\left\langle \mathbf{k}n' \mid v_y \mid \mathbf{k}n\right\rangle}{(\omega_{\mathbf{k}n} - \omega_{\mathbf{k}n'})^2}$$

current operator $\mathbf{j} = -ec\alpha$ (AHE), (charge current operator)

$$\mathbf{j} = \frac{\hbar}{4}\{\beta\Sigma_z, c\alpha_i\}\ \text{(SHE)},$$ (spin current operator)

$$\mathbf{j} = \frac{\hbar}{2}\{\beta L_z, c\alpha\}\ \text{(OHE)}.$$ (orbital current operator)

α, β, Σ are 4×4 Dirac matrices.

4) Application to intrinsic spin Hall effect in semiconductors

[Guo,Yao,Niu, PRL 94, 226601 (2005)]

Spin and orbital angular momentum Hall effects in p-type zincblende semicoductors

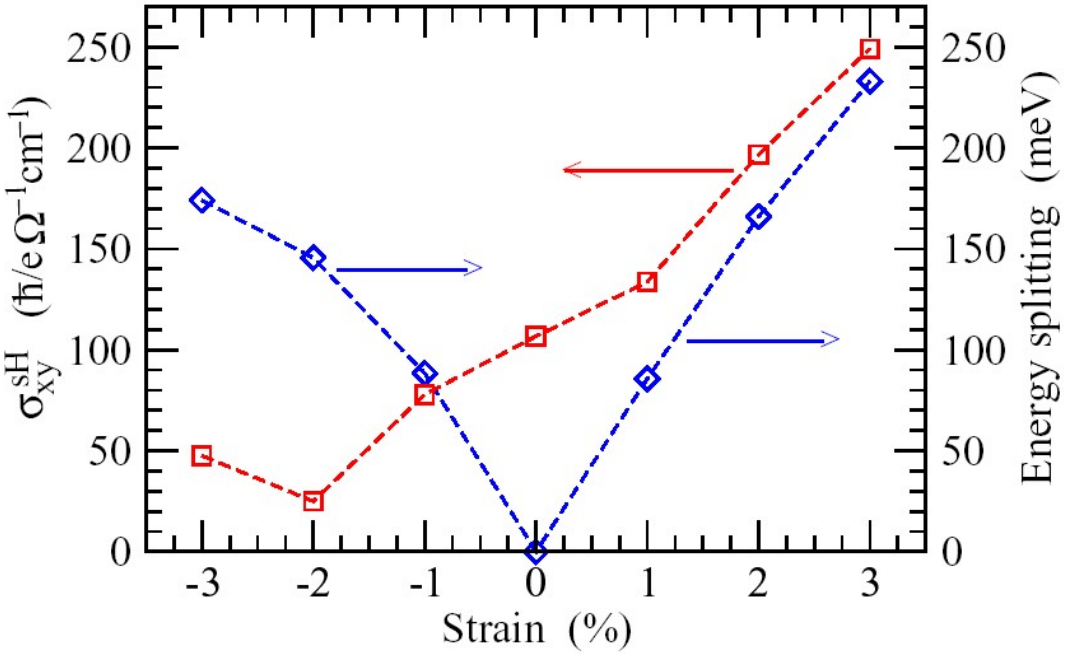

Strain effect

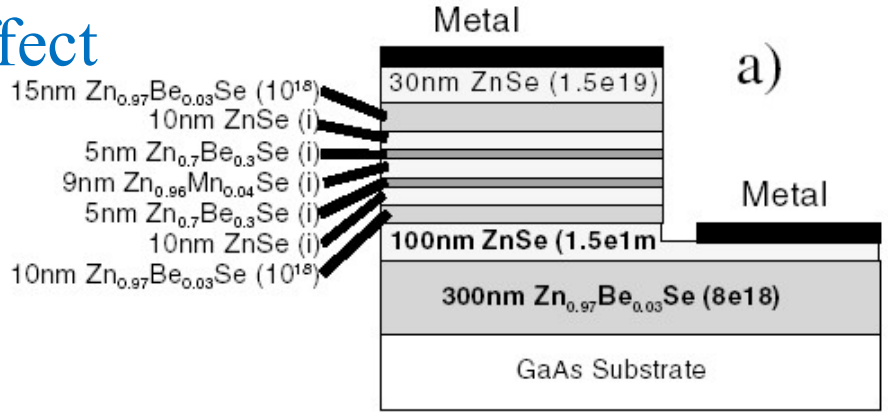

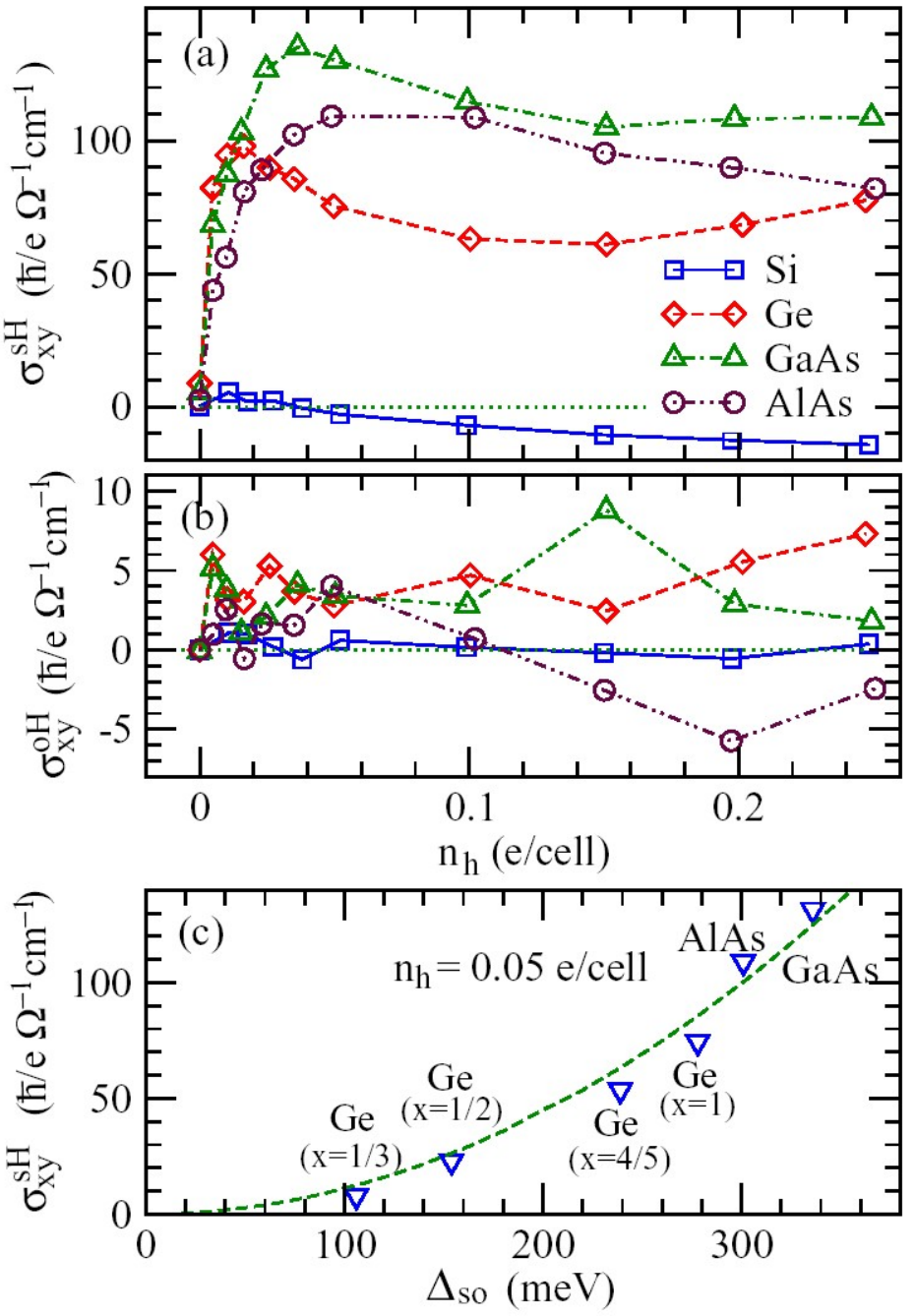

3. Large intrinsic spin Hall effect in platinum metal

Nature 13 July 2006 Vol. 442, P. 176

Direct electronic measurement of the spin Hall effect fcc Al

S. O. Valenzuela[1]† & M. Tinkham[1]

$$R_{SH} = \frac{\Delta R_{SH}}{2}\sin\theta$$

$$\Delta R_{SH} = \frac{P}{t_{Al}}\frac{\sigma_{SH}}{\sigma_c^2}\exp(-L_{SH}/\lambda_{sf})$$

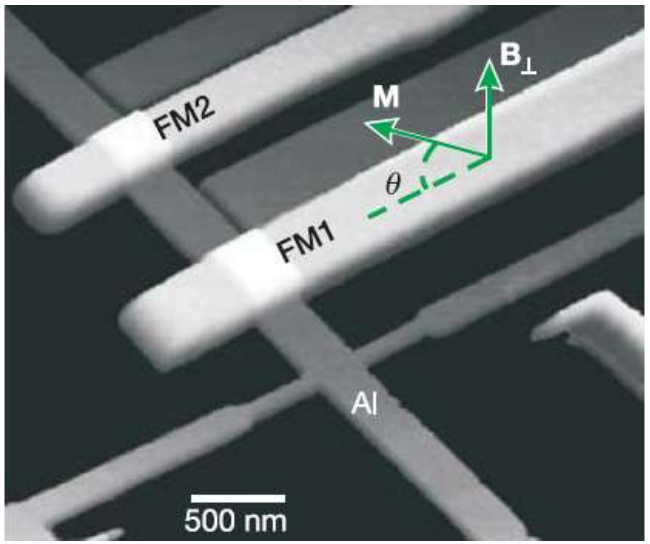

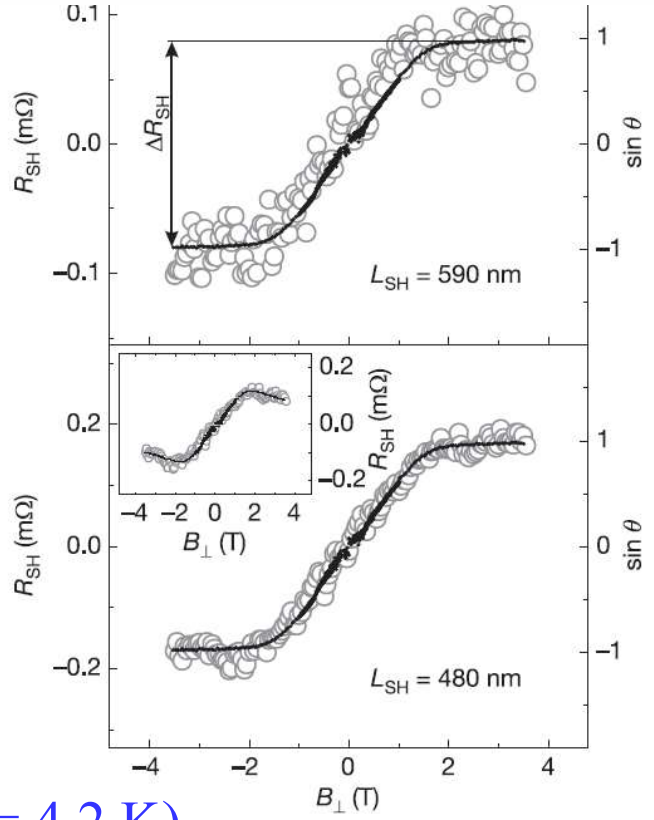

(direct) spin Hall effect

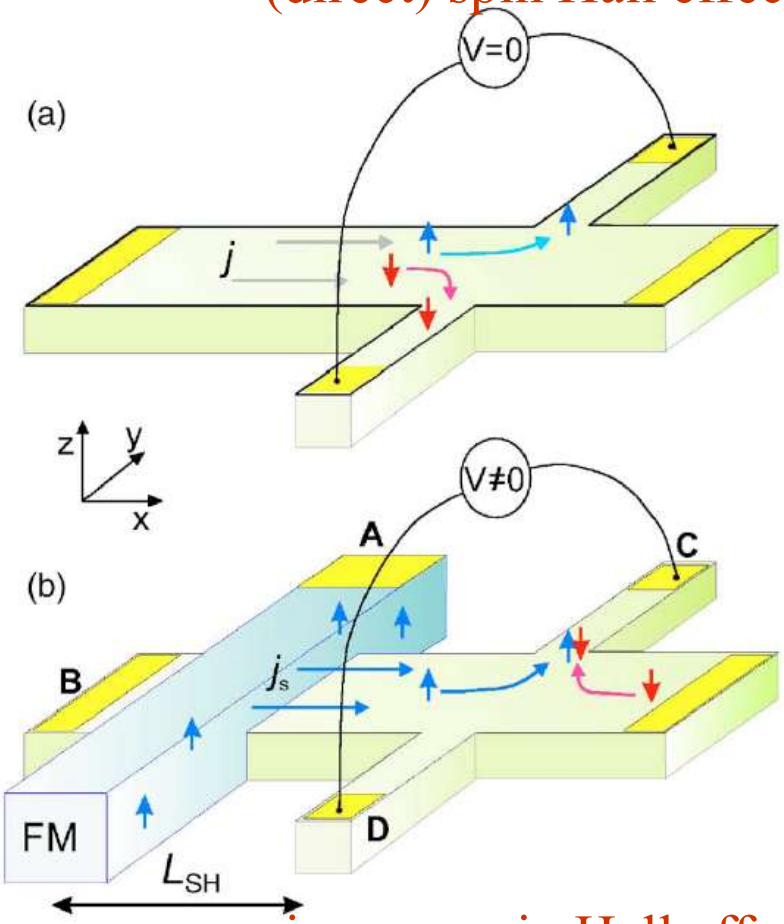

inverse spin Hall effect

$\sigma_{sH} \approx 27\ (\hbar/2e)(\Omega cm)^{-1}\ (T = 4.2\ K)$

spin Hall angle $\theta_{sH} = \sigma_{sH}/\sigma_c \approx 2\times10^{-3}$

spin current $J_s = \theta_{sH}\,(J_c/e)\times\sigma\,(\hbar/2)$

Spin Hall angle θ_{sH} is a measure of the charge current to spin current conversion efficiency

Room-Temperature Reversible Spin Hall Effect

[PRL98, 156601; 98, 139901 (E) (2007)]

T. Kimura,[1,2] Y. Otani,[1,2] T. Sato,[1] S. Takahashi,[3,4] and S. Maekawa[3,4]

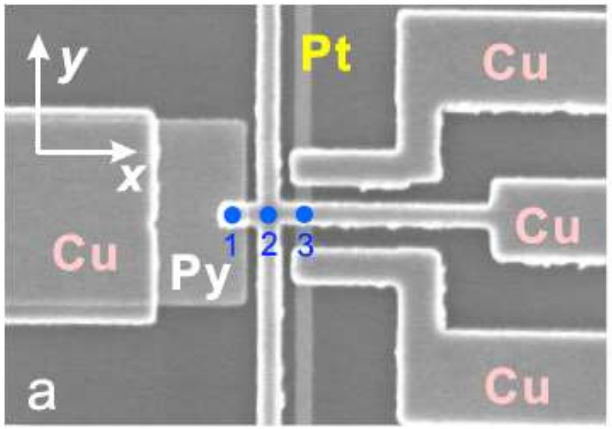

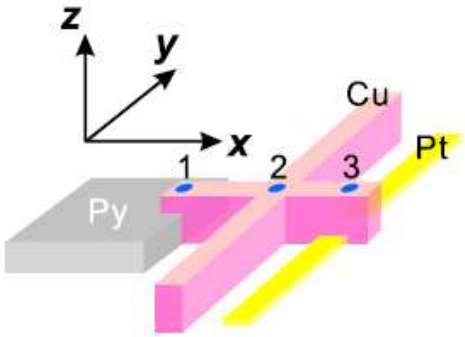

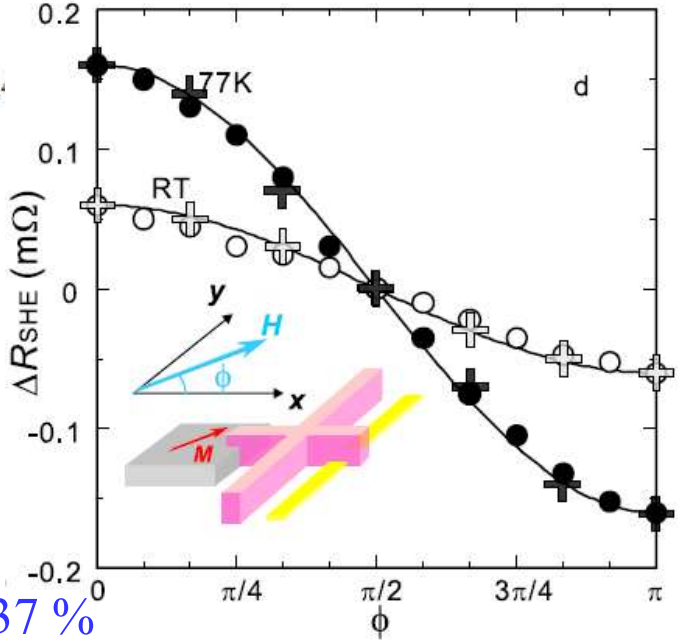

At T= 290 K: $\sigma_{sH} = 240\ (\hbar/2e)(\Omega cm)^{-1}$, $\sigma_c = 65\times10^3\ (\Omega cm)^{-1}$, $\theta_{sH} = 0.37\ \%$

Assumed to be extrinsic!

It is important to understand the detailed mechanism of the SHE in metals because it would lead to the material design of the large SHE at room temperature for spintronics. To this end, first-principles band theoretical calculations for real metal systems is essential.

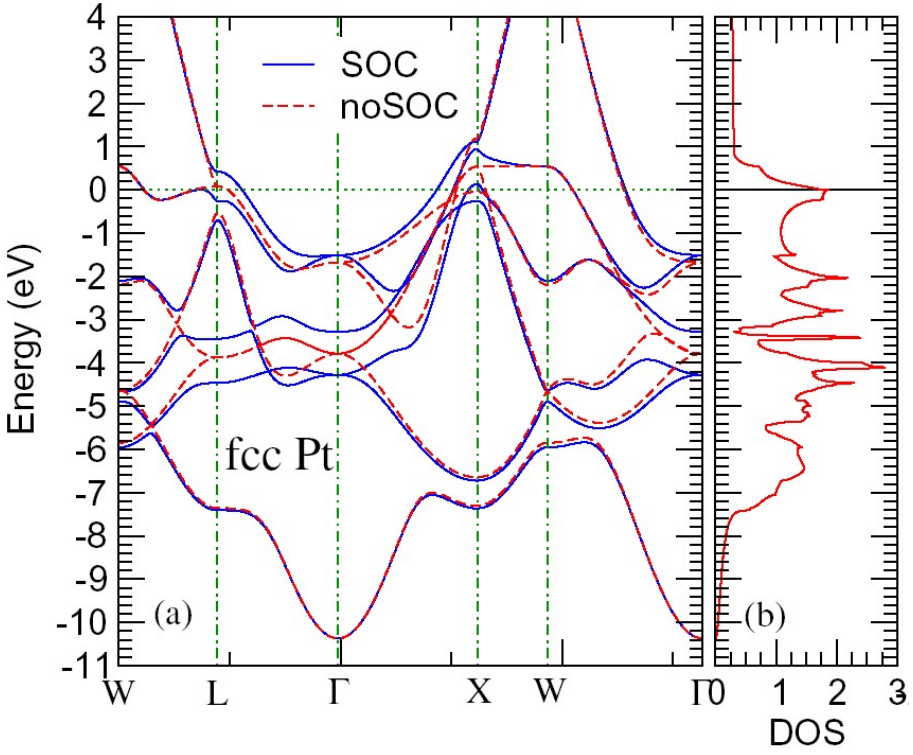

Large intrinsic spin Hall effect in platinum

[Guo, Murakami, Chen, Nagaosa, PRL100, 096401 (2008)]

Ab initio calculations:

Al: $\sigma_{sH} = 34\ (\hbar/2e)(\Omega cm)^{-1}$

σ_{sH} (exp., 4.2K) $\approx 27\ (\hbar/2e)(\Omega cm)^{-1}$

[Valenzuela, Tinkham, Nature 442, 176 (2006)]

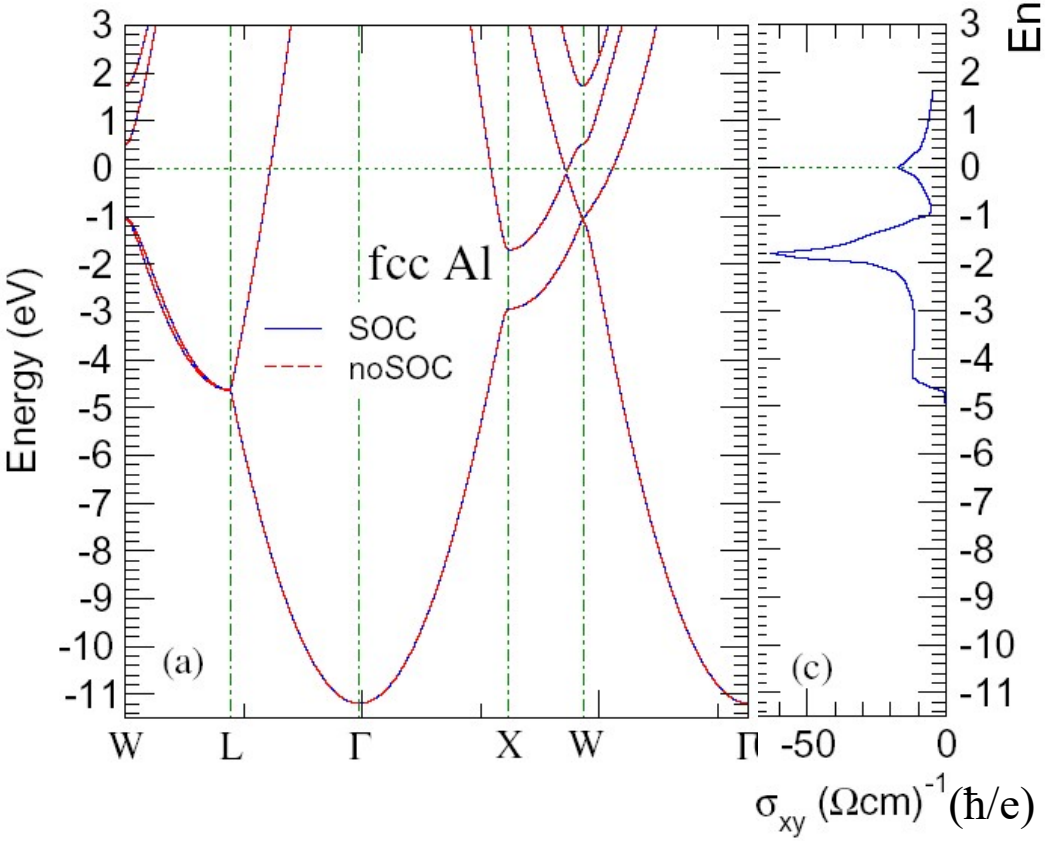

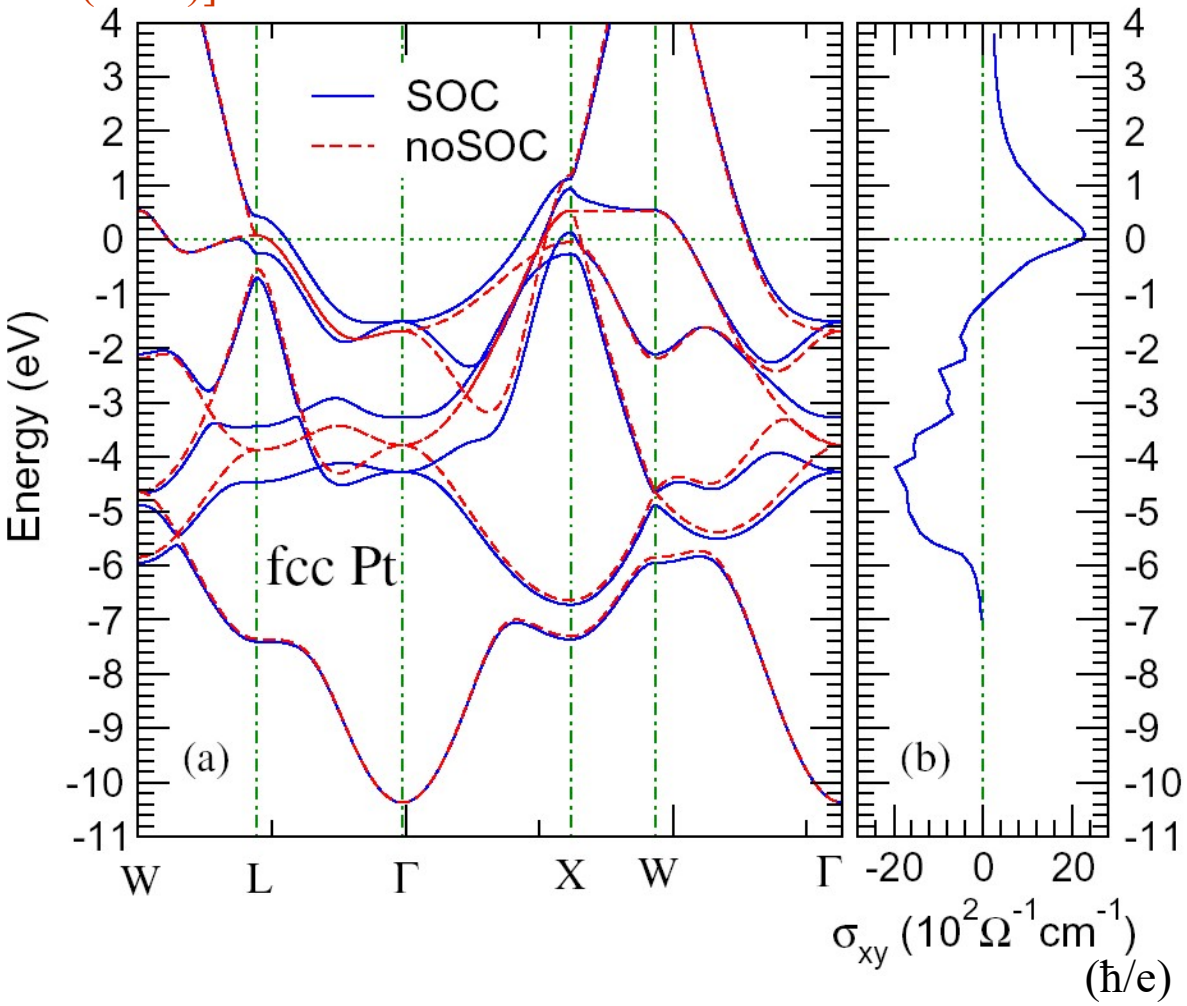

Pt: $\sigma_{sH} = 4400\ (\hbar/2e)(\Omega cm)^{-1}$

$$\sigma_{sH} = -\frac{e}{\hbar}\sum_{\mathbf{k}}\Omega^{z}(\mathbf{k}) = \frac{e}{\hbar}\sum_{\mathbf{k}}\sum_{n} f(\varepsilon_n(\mathbf{k}))\Omega_n^{z}(\mathbf{k}), \quad \Omega_n^{z}(\mathbf{k}) = \sum_{n'\neq n}\frac{2\,\mathrm{Im}\left\langle \mathbf{k}n \mid j_x^z \mid \mathbf{k}n'\right\rangle\left\langle \mathbf{k}n' \mid v_y \mid \mathbf{k}n\right\rangle}{(\omega_{\mathbf{k}n}-\omega_{\mathbf{k}n'})^2}$$

spin Berry curvature

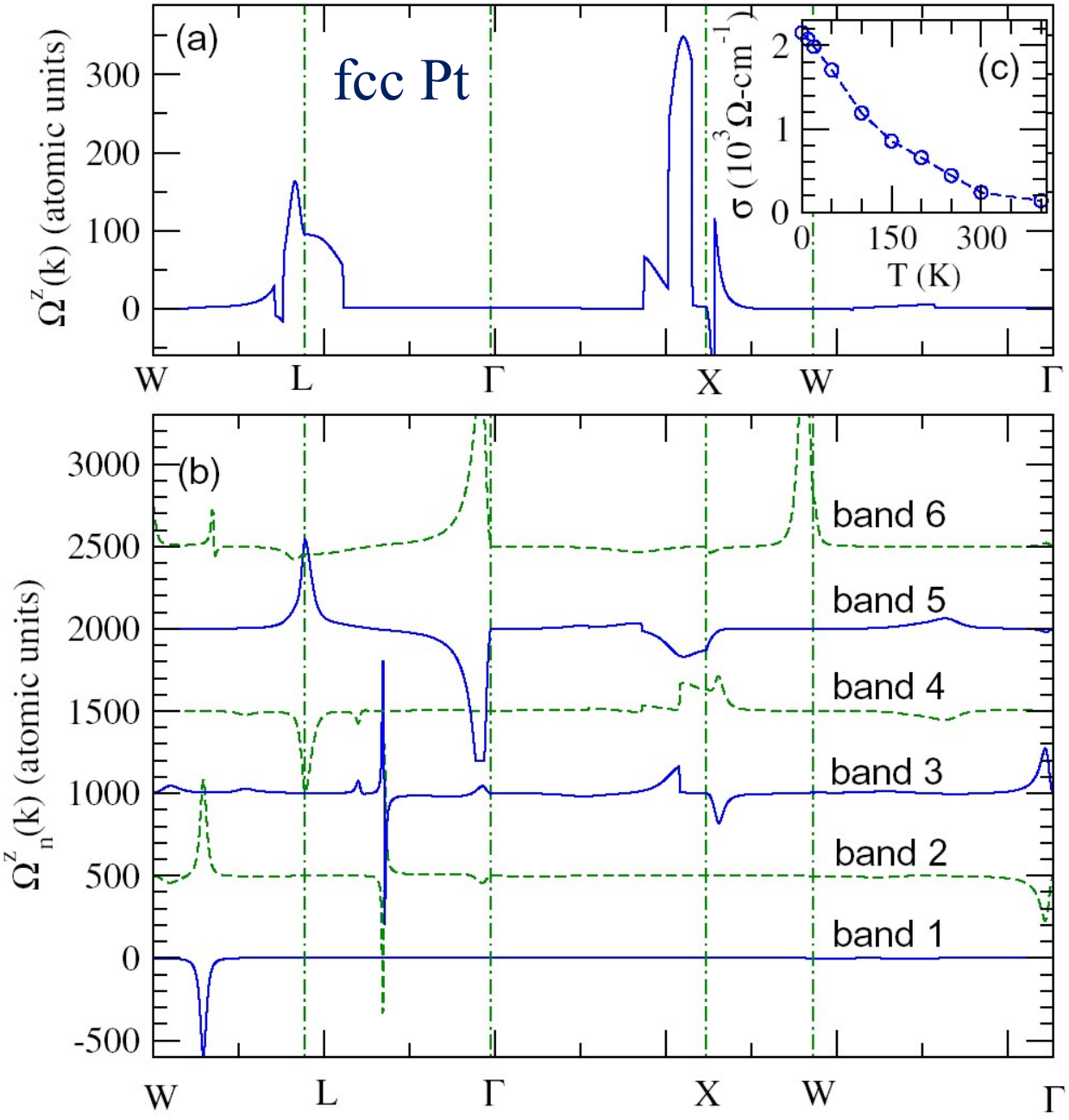

Theory:

σ_{sH} (0K) = 4400 (ħ/2e)(Ωcm)$^{-1}$

Experiments:

σ_{sH} (290K) = 240 (ħ/2e)(Ωcm)$^{-1}$

θ_{sH} = 0.37 %

[Kimura et al PRL98, 156601 (2007)]

σ_{sH} (10K) = 1700 (ħ/2e)(Ωcm)$^{-1}$

θ_{sH} = 2.1 %

[Morota et al, PRB 83, 174405 (2011)]

σ_{sH} (290K) = 3400 (ħ/2e)(Ωcm)$^{-1}$

θ_{sH} = 6.8 %

[Liu et al, PRL 106, 036601 (2011)]

Subsequently, many measurements on the SHE in metals were carried out. The consensus is that Pt has the largest spin Hall conductivity (SHC) and its SHC is mainly intrinsic. [Hoffmann, IEEE Trans. Magn. 49 (2013) 5172]

Thus, Pt has been widely used as spin current generator and detector in recent novel spin transport experiments, e.g.,

Spin Seebeck effect (spin caloritronics),
[Uchida et al., Nature 455, 778 (2008)]

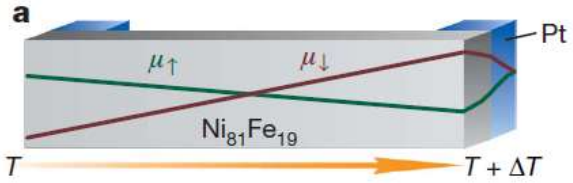

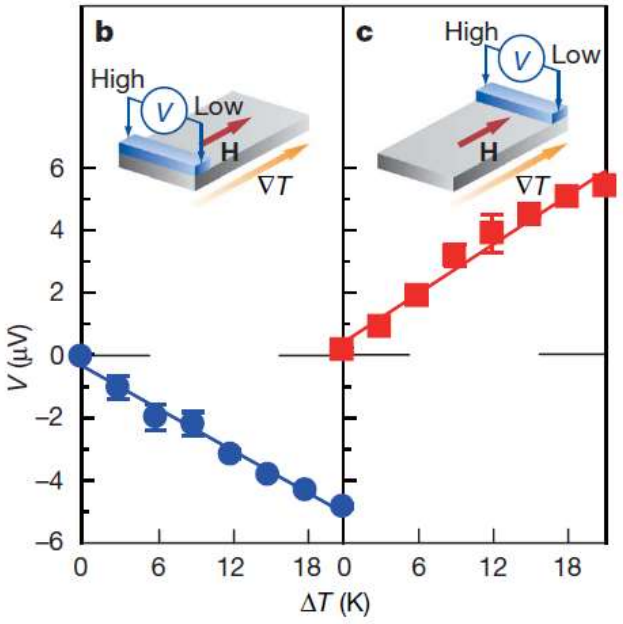

spin Hall switching
[Miron et al., Nature 476, 189 (2011)]

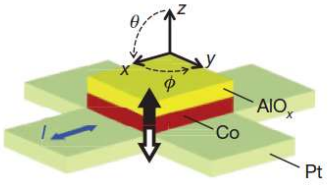

(electrical writing)

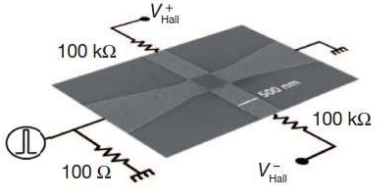

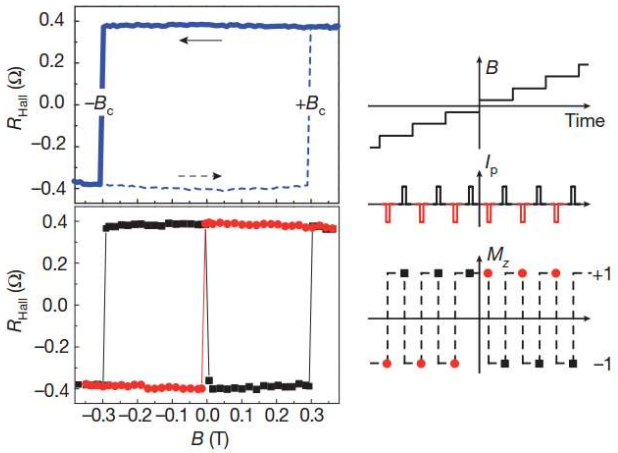

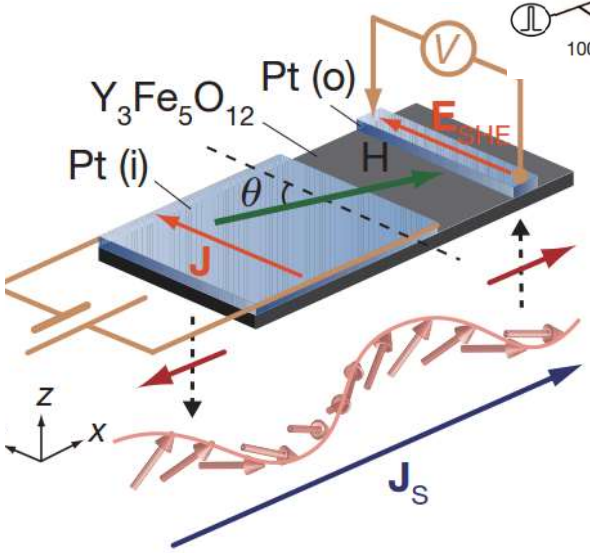

Injection and detection of spin-wave spin current
[Kajiwara et al., Nature 464, 262 (2010)]

III. Multi-orbital Kondo effect in Fe-doped gold

Intrinsic spin Hall effect in pure Au

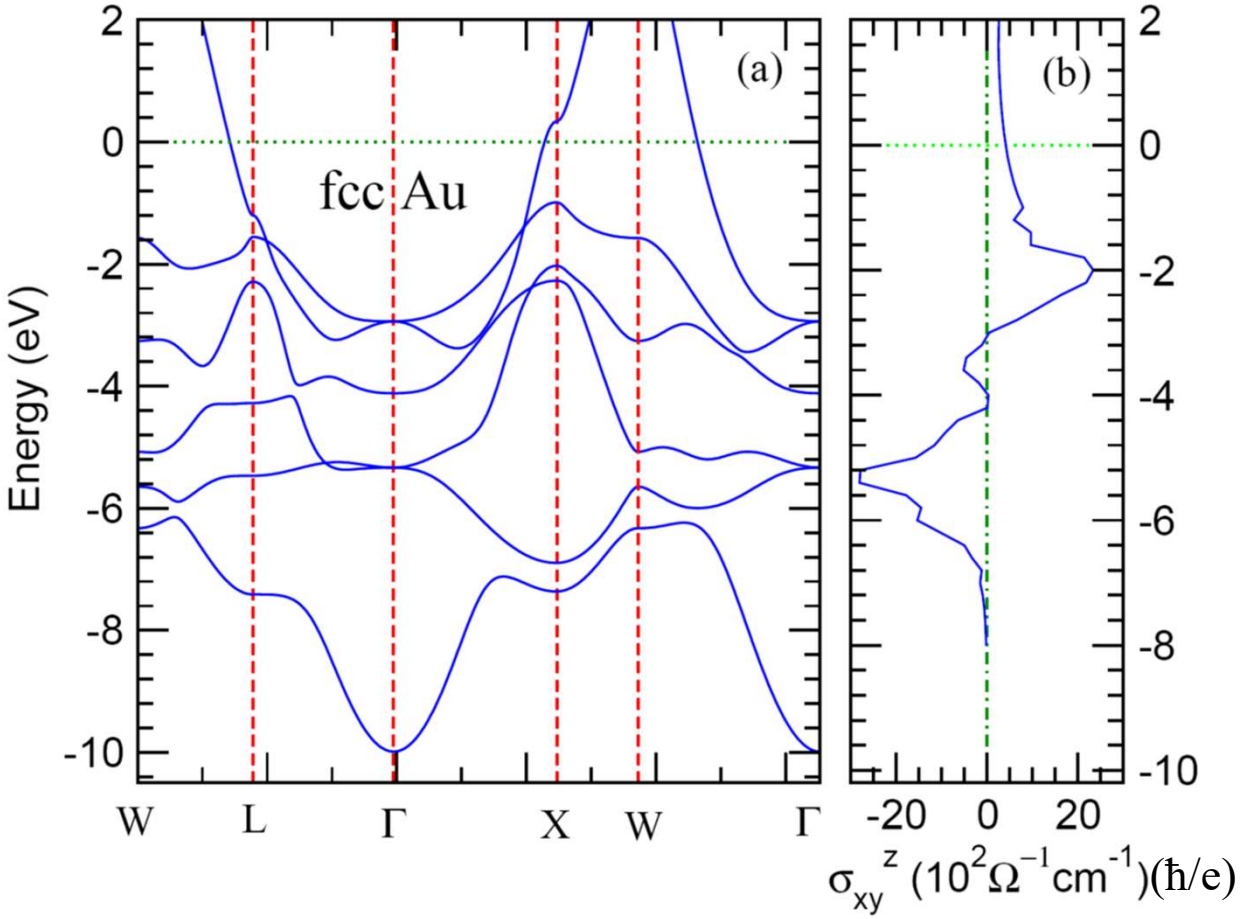

σ_{sH} = 830 (ħ/2e)($(\Omega cm)^{-1}$

[Guo, JAP 105, 07C701 (2009)]

σ_{sH} = 882 (ħ/2e)$(\Omega cm)^{-1}$
σ_c = 252×10^3 $(\Omega cm)^{-1}$
θ_s = 0.35 %

[Mosendz et al., PRB 82 (2010) 214403]

1. Giant spin Hall effect in perpendicularly spin-polarized FePt/Au devices [Seki, et al., Nat. Mater. 7 (2008)125]

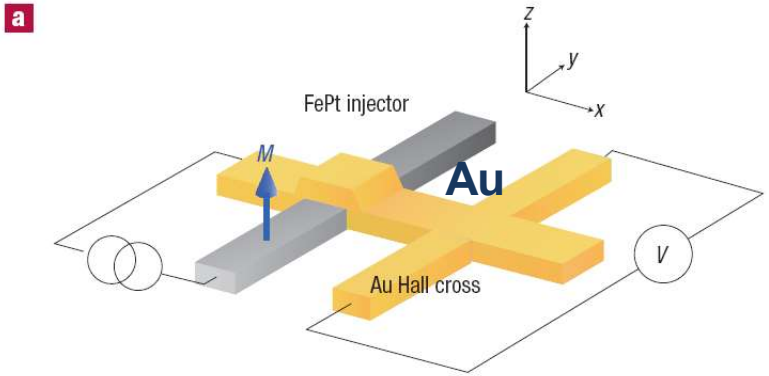

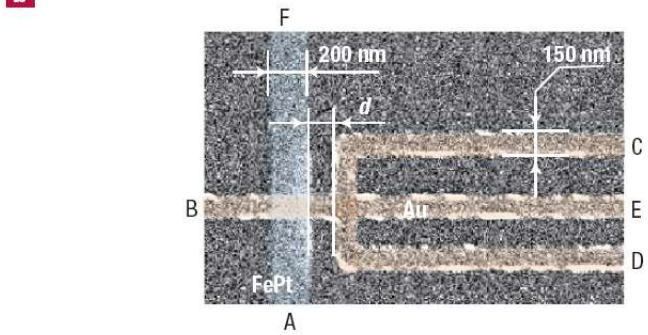

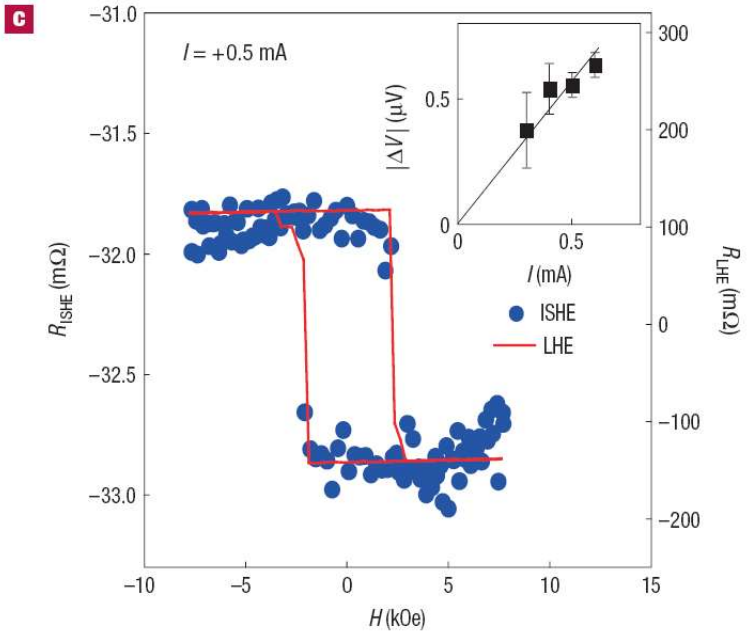

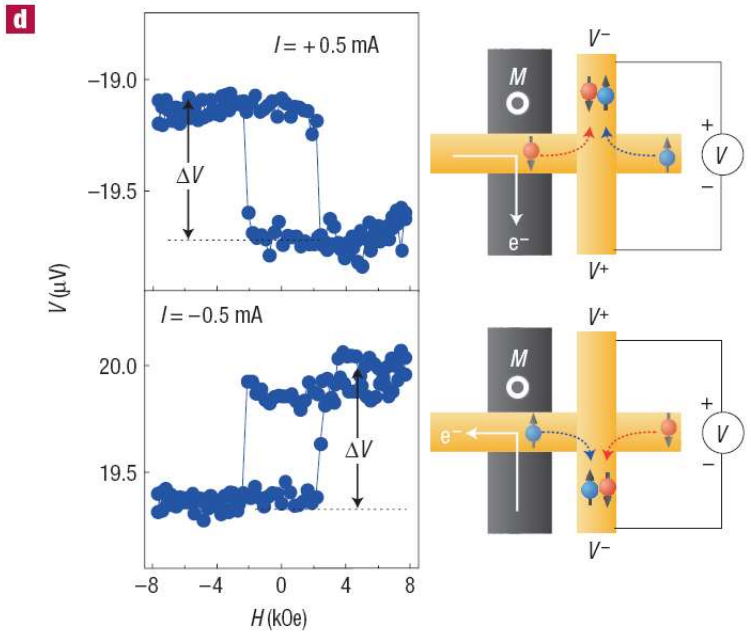

What is the origin of giant spin Hall effect in gold Hall bars?

Due to defect and impurity?

Possible impurities:
(a) Au vacancy
(b) Pt impurity
(c) Fe impurity

$$\Delta R_{ISHE} = 2\theta_s \frac{\rho_{Au}}{t_{Au}} P \exp(-d/\lambda_{Au})$$ spin Hall angle $\theta_s = \frac{\sigma_{sH}}{\sigma_{xx}} \approx 0.1$ at RT

σ_{sH} =42000 (ħ/2e)($(\Omega cm)^{-1}$

2. Multi-orbital Kondo effect

1) The idea

Results of FLAPW calculations:

(a) the change in DOS in the 5d bands.

(b) the DOS change is near -1.5 eV.
Nonmagnetic in (a) and (b)

(c) A peak in DOS at the Fermi level and magnetic.

[Guo, Maekawa, Nagaosa, PRL 102, 036401 (2009)]

Proposal: Multi-orbital Kondo effect in Fe impurity in gold, leading to the enhanced spin Hall effect by resonant skew-scattering.

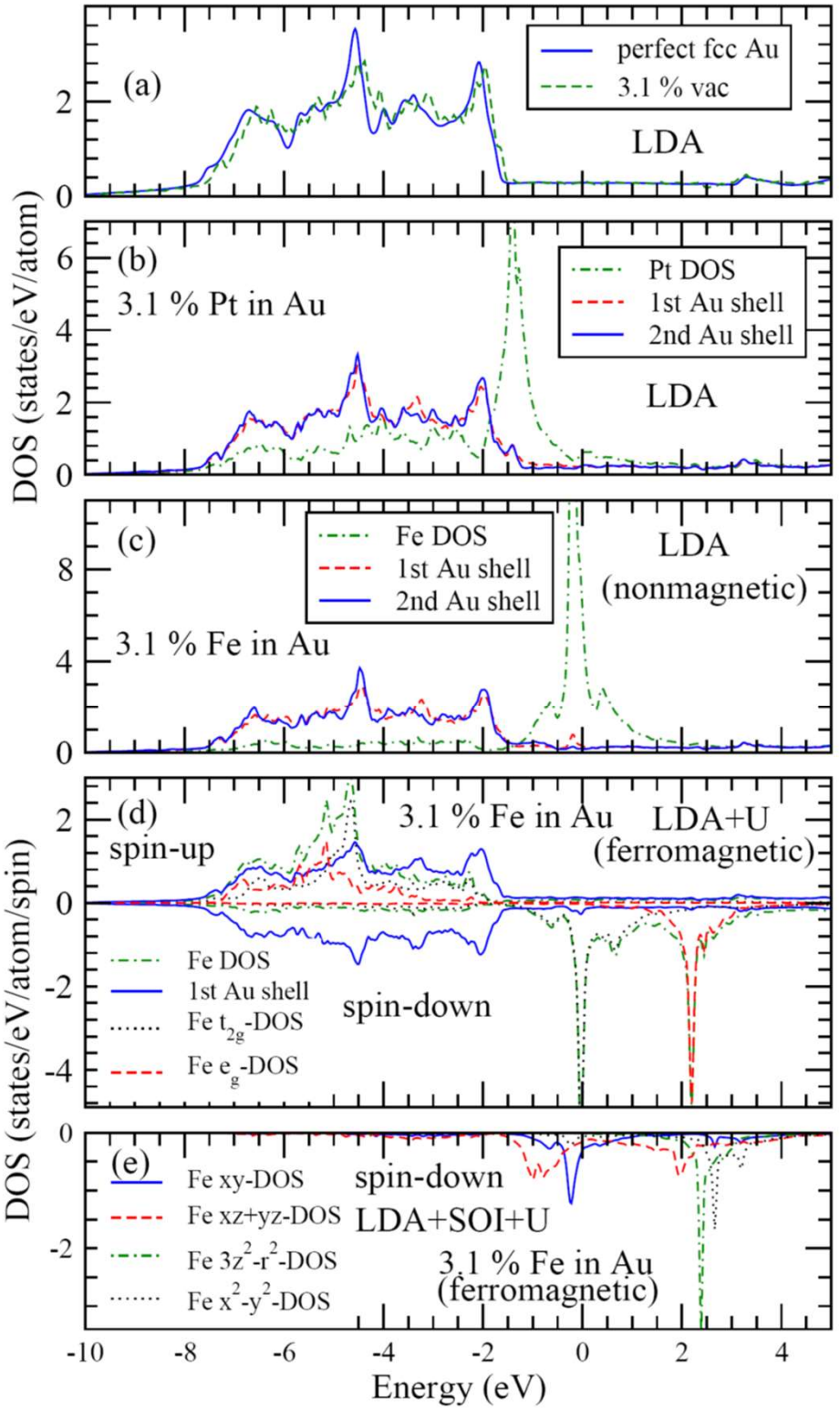

2) Introduction to Kondo effect

(A classic many-body phenomenon in condensed matter physics)

(1) Resistivity abnormality in Au with dilute magnetic impurities discovered by de Haas et al. in 1930's.

Jun Kondo (1930 -)

Strong coupling

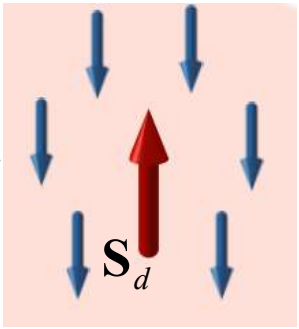

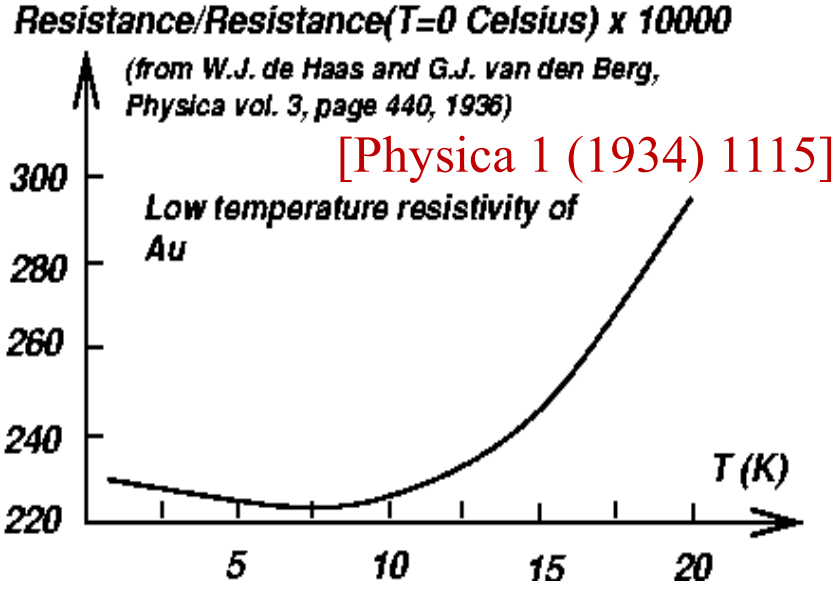

[Physica 1 (1934) 1115]

(2) Kondo proposed a (Kondo) model and solved it in the 3rd-order perturbation theory to explain the phenomenon in 1960's.

[Prog. Theo. Phys. 32 (1964) 37]

$$H = \sum_{\mathbf{k}\sigma} \varepsilon_k c^{\dagger}_{\mathbf{k}\sigma} c_{\mathbf{k}\sigma} + J\boldsymbol{\sigma}(0)\cdot\mathbf{S}_d \qquad (J>0,\ S_d = 1/2)$$

$$\rho(T) = C_{imp}\rho_0 + aT + C_{imp}\rho_1 \ln(\mu/T),$$

$$T_{\min} = (\rho_1/5a)^{1/5} C_{imp}^{1/5} \approx T_K \ \text{(Kondo temperature)}$$

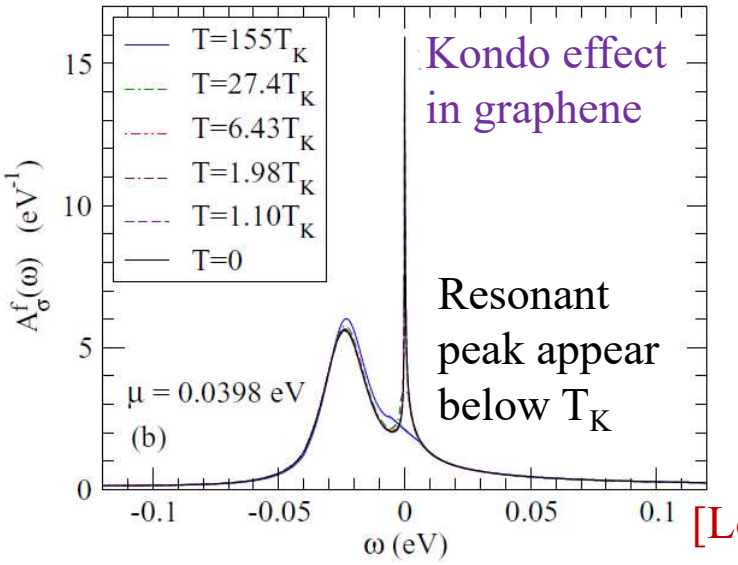

[Lo, Guo, Anders, PRB 89 (2014) 195424]

3) Enhanced spin Hall angle due to skew scattering

Textbook calculation [Bethe & Jackiw(1986) Intermediate QM]

[Engel, Halperin, Rashba, PRL 95, 166605 (2009)]

[Guo, Maekawa, Nagaosa, PRL 102, 036401 (2009)]

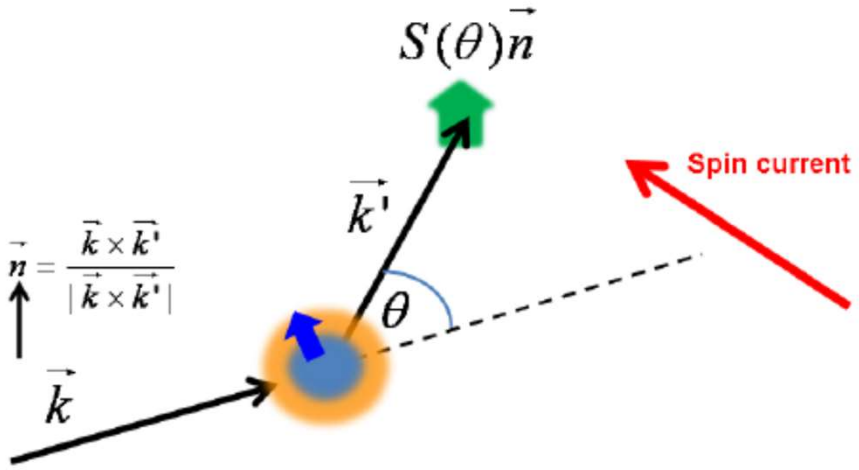

FIG. 1: (color online) The skew scattering due to the spin-orbit interaction of the scatterer and the spin unpolarized electron beam with wavevector $\vec{k}$ with the angle θ with the spin polarization $S(\theta)\vec{n}$ with $\vec{n} = (\vec{k}\times\vec{k}')/|\vec{k}\times\vec{k}'|$.

scattering amplitudes

$$f_\uparrow(\theta) = f_1(\theta)|\uparrow\rangle + ie^{i\varphi} f_2(\theta)|\downarrow\rangle$$
$$f_\downarrow(\theta) = f_1(\theta)|\downarrow\rangle - ie^{-i\varphi} f_2(\theta)|\uparrow\rangle$$

skewness function

$$S(\theta) = \frac{2\mathrm{Im}[f_1^*(\theta) f_2(\theta)]}{|f_1(\theta)|^2 + |f_2(\theta)|^2}$$

spin Hall angle

$$\gamma_S = \frac{\int d\Omega I(\theta) S(\theta) \sin\theta}{\int d\Omega I(\theta)(1-\cos\theta)}$$

$$f_1(\theta) = \sum_l \frac{P_l(\cos\theta)}{2ik}\left[(l+1)\left(e^{2i\delta_l^+} - 1\right) + l\left(e^{-2i\delta_l^-} - 1\right)\right]$$

$$f_2(\theta) = \sum_l \frac{\sin\theta}{2ik}\left(e^{2i\delta_l^+} - e^{2i\delta_l^-}\right)\frac{d}{d\cos\theta}P_l(\cos\theta).$$

Numerical estimate of spin Hall angle

[Guo, Maekawa, Nagaosa, PRL 102, 036401 (2009)]

$$\theta_s \cong -\frac{3\delta_1(\cos 2\delta_2^+ - \cos 2\delta_2^-)}{9\sin^2\delta_2^+ + 4\sin^2\delta_2^- + 3[1-\cos 2(\delta_2^+ - \delta_2^-)]}$$

TABLE I. Down-spin occupation numbers of the $3d$ orbitals of the Fe impurity in Au from LDA + U calculations. The calculated magnetic moments are $m_s^{\mathrm{Fe}} = 3.39\mu_B$ and $m_s^{\mathrm{tot}} = 3.32\mu_B$ without SOI, as well as $m_s^{\mathrm{Fe}} = 3.19\mu_B$, $m_o^{\mathrm{Fe}} = 1.54\mu_B$, and $m_s^{\mathrm{tot}} = 3.27\mu_B$ with SOI.

(a)	xy	xz	yz	$3z^2 - r^2$	$x^2 - y^2$
No SOI	0.459	0.459	0.459	0.053	0.053
SOI	0.559	0.453	0.453	0.050	0.128
(b)	$m = -2$	$m = -1$	$m = 0$	$m = 1$	$m = 2$
No SOI	0.256	0.459	0.053	0.459	0.256
SOI	0.138	0.087	0.050	0.819	0.549

$\theta_s \cong \delta_1 \approx 0.1$

Occupation numbers are related to the phase shifts through generalized Friedel sum rule.

Physics *Physics* **2**, 6 (2009)

Piers Coleman
Department of Physics and Astronomy, Rutgers Univers

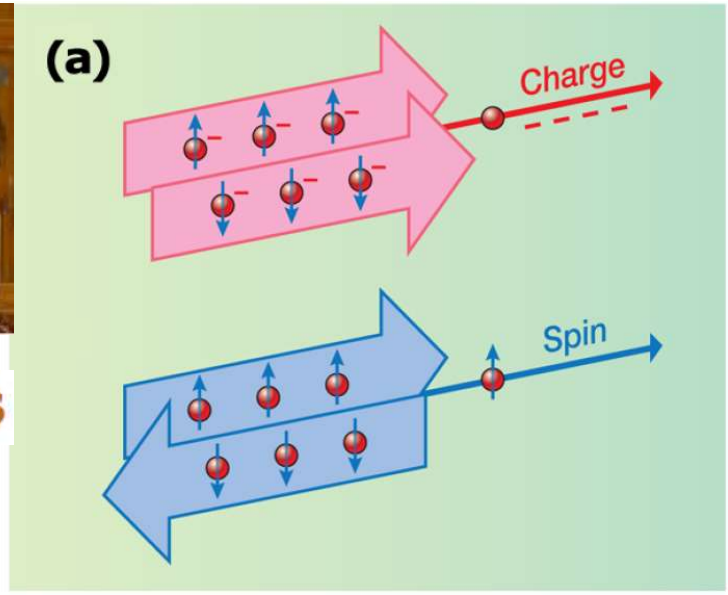

Viewpoint Lending an iron hand to spintronics

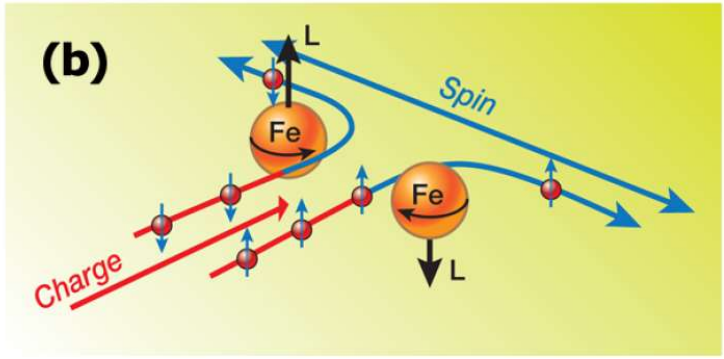

"If Guo *et al.* are right in their interpretation, the observation of a giant spin Hall effect resulting from the Kondo effect will add a curious new twist to this story. The history of the Kondo effect stretches back over seventy-five years. Despite its long history, the detailed Kondo physics of iron remains a controversial subject."

"This is a fascinating state of affairs—a wonderful example of the synergy that is possible between electronics applications and condensed-matter physics. … … This could be a very exciting and unexpected turn in the long-standing story of the Kondo effect of iron in gold."

A Viewpoint on:
Enhanced Spin Hall Effect by Resonant Skew Scattering in the Orbital-Dependent Kondo Effect
Guang-Yu Guo, Sadamichi Maekawa and Naoto Nagaosa
Phys. Rev. Lett. **102**, 036401 (2009) – Published January 20, 2009

Influence of Fe Impurity on Spin Hall Effect in Au

Isamu Sugai[1], Seiji Mitani[2], and Koki Takanashi[1]

[1]Institute for Materials Research, Tohoku University, Sendai 980-8577, Japan
[2]National Institute for Materials Science, Tsukuba 305-0047, Japan

We investigated the influence of Fe impurity on spin Hall effect in Au using multi-terminal devices consisting of an FePt perpendicular spin polarizer and a Au Hall cross with different Fe impurity concentrations. As the Fe impurity concentration was increased in the range of 0–0.95 at.%, the resistivity of Au doped with Fe increased and the spin diffusion length decreased from 35 nm to 27 nm. On the other hand, the spin Hall angle for Au doped with Fe, evaluated from the spin injector-Hall cross distance dependence of spin Hall signals, was approximately 0.07, independent of the Fe concentration. The experimental results provide important information for understanding the mechanism of the large spin Hall effect.

Skew scattering
θ_s ~0.07 ,
independent of
Fe concentration.

PARAMETERS OF $P_{\underline{\mathrm{AuFe}}}$, $R_s^{\underline{\mathrm{AuFe}}}$, $\lambda_{\underline{\mathrm{AuFe}}}$, P AND α_H OBTAINED FOR THE PRESENT FePt/Au DEVICES

	$\rho_{\underline{\mathrm{AuFe}}}$ [μΩ·cm]	$\lambda_{\underline{\mathrm{AuFe}}}$ [nm]	$R_s^{\underline{\mathrm{AuFe}}}$ [Ω]	P	α_H
Non-doped Au	3.6	35 ± 4	1.1	0.038	0.07 ± 0.02
$Au_{99.58}Fe_{0.42}$	4.3	33 ± 3	1.3	0.034	0.07 ± 0.01
$Au_{99.05}Fe_{0.95}$	7.0	27 ± 3	1.7	0.027	0.07 ± 0.03

IV. Quantum topological Hall effect in chiral antiferromagnets

1. Quantum anomalous Hall effect

1) Ordinal Hall Effect [Hall 1879]

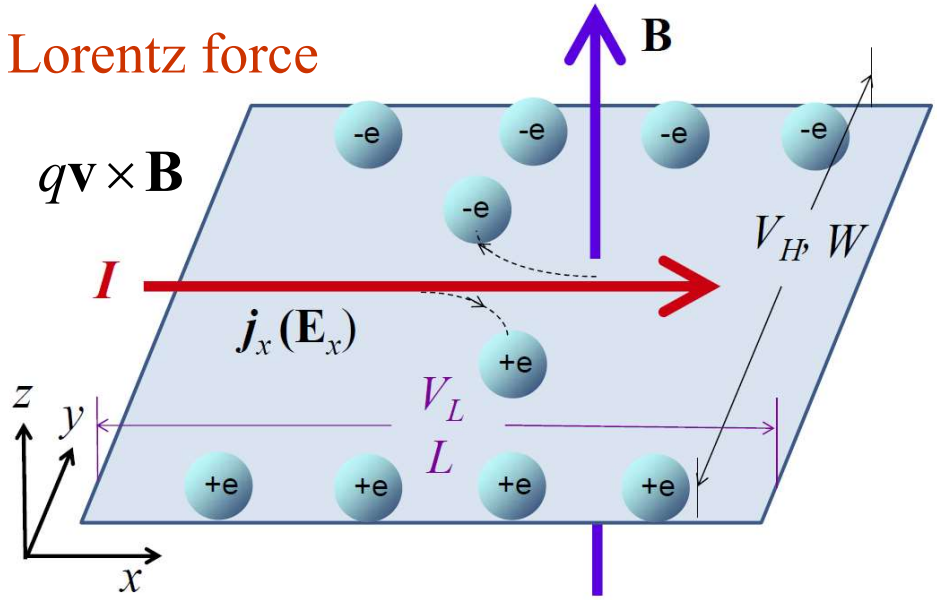

$$R_L = V_L / I = (E_x L)/(j_x W) = \rho_{xx}(L/W)$$

$$R_H = V_H / I = (E_y W)/(j_x W) = \rho_{xy} = (1/nq)B$$

Edwin H. Hall (1855-1938)

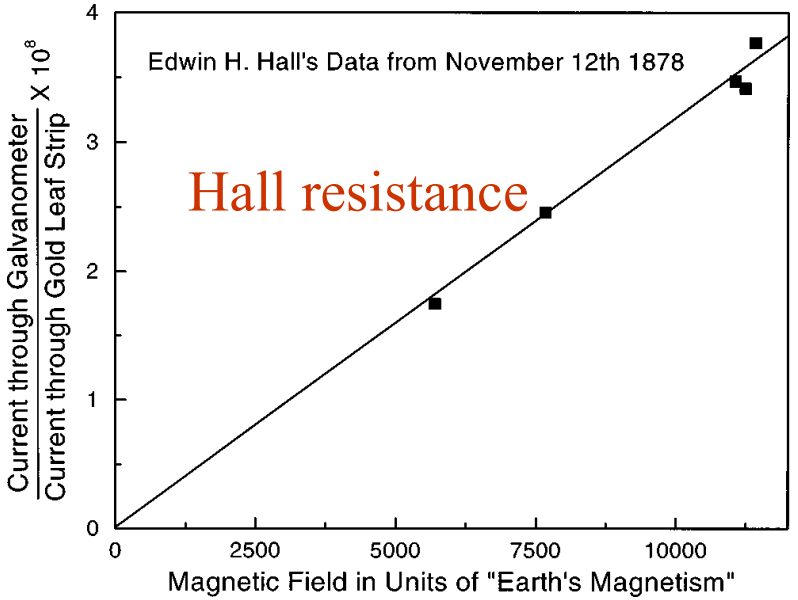

2) (Integer) quantum Hall Effect [von Klitzing et al., 1980]

In 1980, von Klitzing et al discovered QHE. [PRL 45, 494]

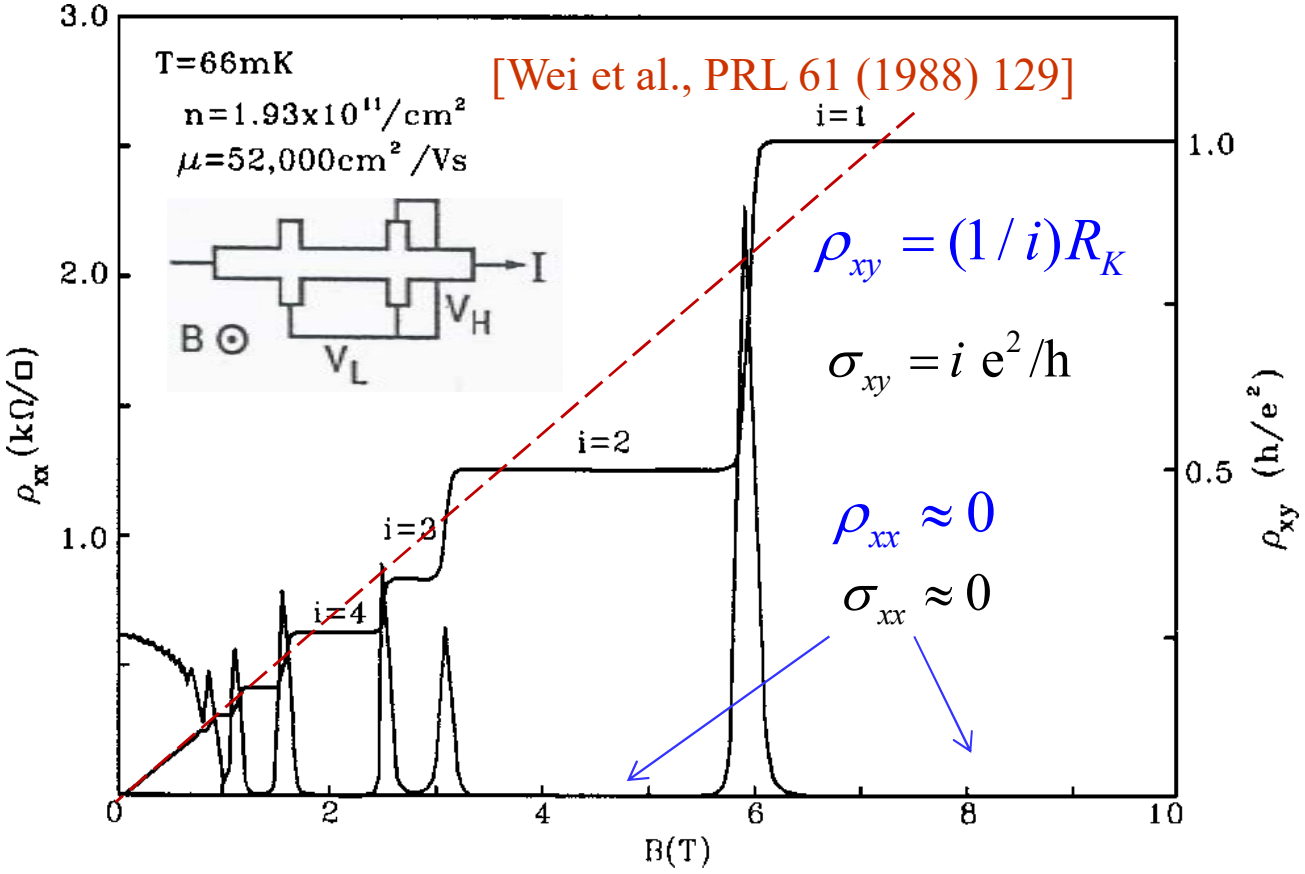

Klaus von Klitzing (1943-present)

von Klitzing constant

$R_K = 1\ h/e^2$

$= 25812.807557(18)\ \Omega$

Conductance quantum

$\sigma_0 = 1/R_K = 1\ e^2/h$

$\rho_{xx} \approx 0$, superconducting states ($\sigma_{xx} \approx \infty$)?

$$\boldsymbol{\rho} = \begin{pmatrix} 0 & \rho_{xy} \\ -\rho_{xy} & 0 \end{pmatrix}, \quad \boldsymbol{\sigma} = [\boldsymbol{\rho}]^{-1} = \begin{pmatrix} 0 & -1/\rho_{xy} \\ 1/\rho_{xy} & 0 \end{pmatrix},$$

$\sigma_{xy} = -1/\rho_{xy} = i\sigma_0, \ \sigma_{xx} = 0,$ they are insulating phases.

Formation of discrete Landau levels

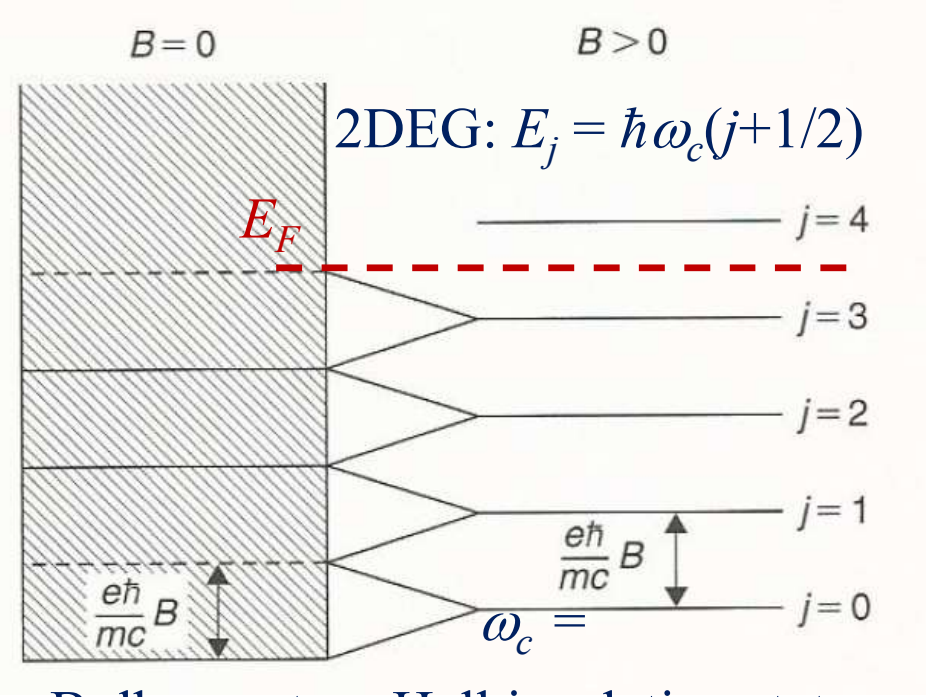

Bulk quantum Hall insulating state

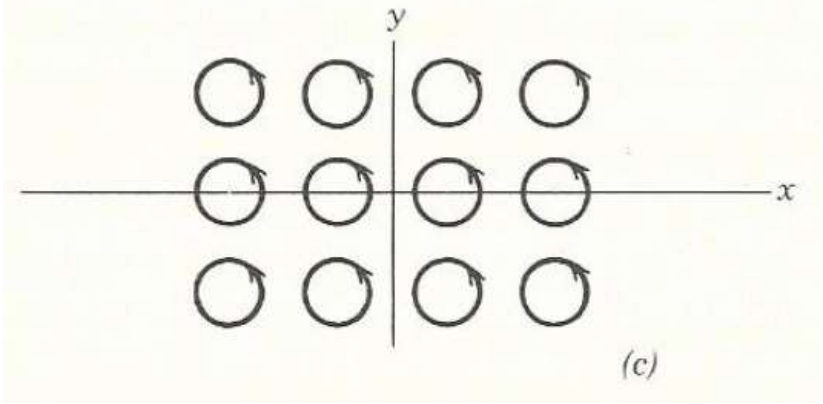

Quantization of Hall conductance

due to topological invariance

[PRL49, 405 (1982)]

$$\sigma_{xy} = n\frac{2e^2}{h},\ n = \text{Chern \#},$$

$$n = \frac{1}{2\pi}\sum_i \int_{\text{2D BZ}} dk_x dk_x \Omega_z^i(\mathbf{k})$$

David Thouless (1934-)

2D BZ is a torus.
Chern theorem:

$$\int_{\text{2D BZ}} dk_x dk_x \Omega_z(\mathbf{k}) = \int_S \Omega(\mathbf{k})\cdot dS = 2\pi C.$$

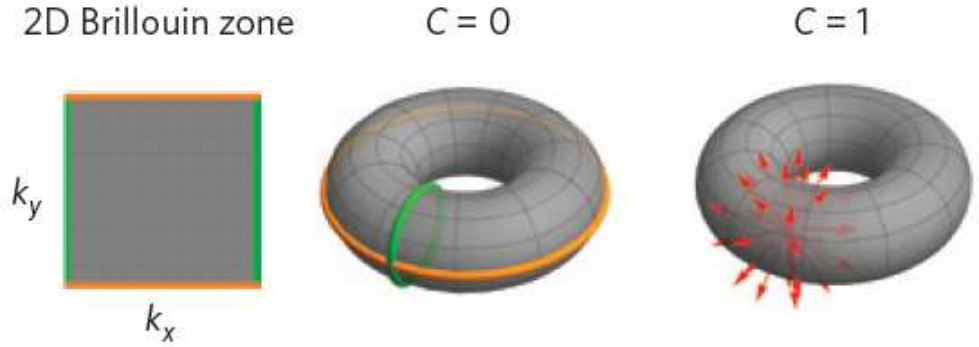

QH phases are the first discovered topological phases of quantum matter; QH systems are the first topological insulators with broken time-reversal symmetry. Topological invariant is Chern number.

Q: A nonzero conductance in an insulating system! How can it be possible?

A: Existence of conducting edge states (modes)

To do measurements, a finite size sample
and hence boundaries must be created.

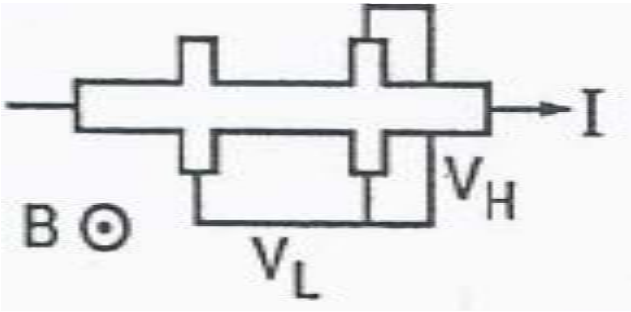

Bending of the LL

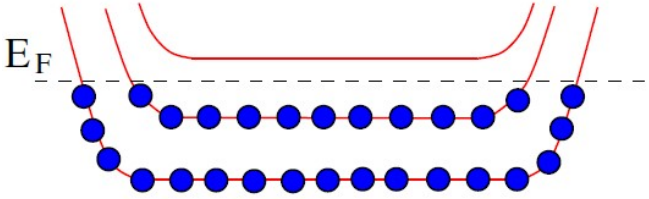

(a) Bulk-edge correspondence theorem

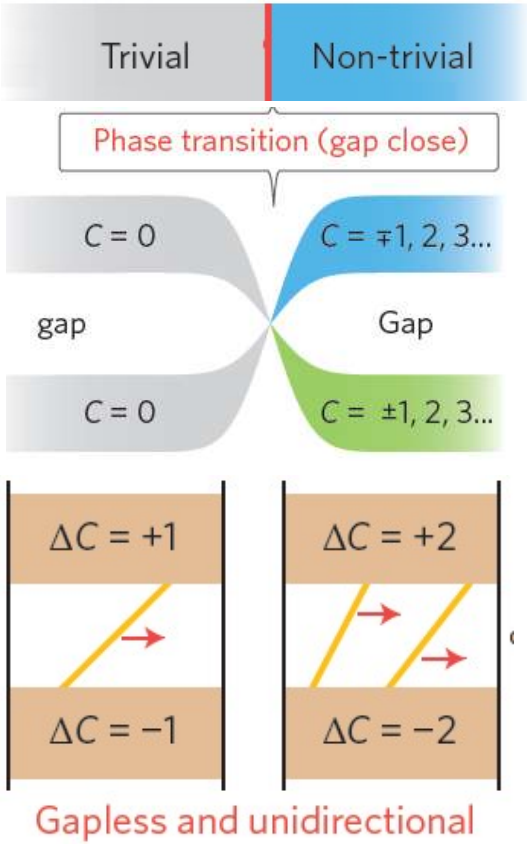

When crossing the boundary between two different Chern insulators, the band gap would close and open again, i.e., metallic edge states exist at the edge whose number is equal to the difference in Chern number.

(b) Explicit energy band calculations

[Hatsugai, PRL 71 (1993) 3697]

IQHE is an intriguing phenomenon due to the occurrence of bulk topological insulating phases with dissipationless conducting edge states in the Hall bars at low temperatures and under strong magnetic field. Hall resistance is so precisely quantized that it can be used to determine the fundamental constants and robust metallic edge state is useful for low-power consuming nanoelectronics and spintronics.

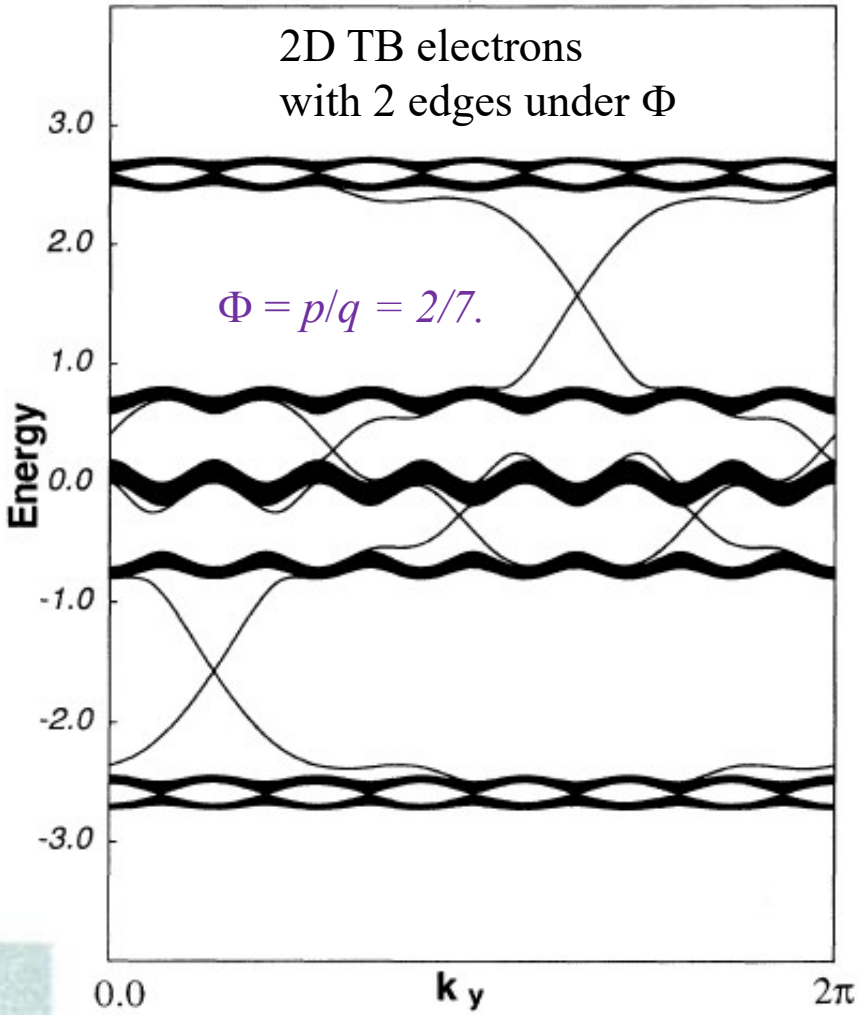

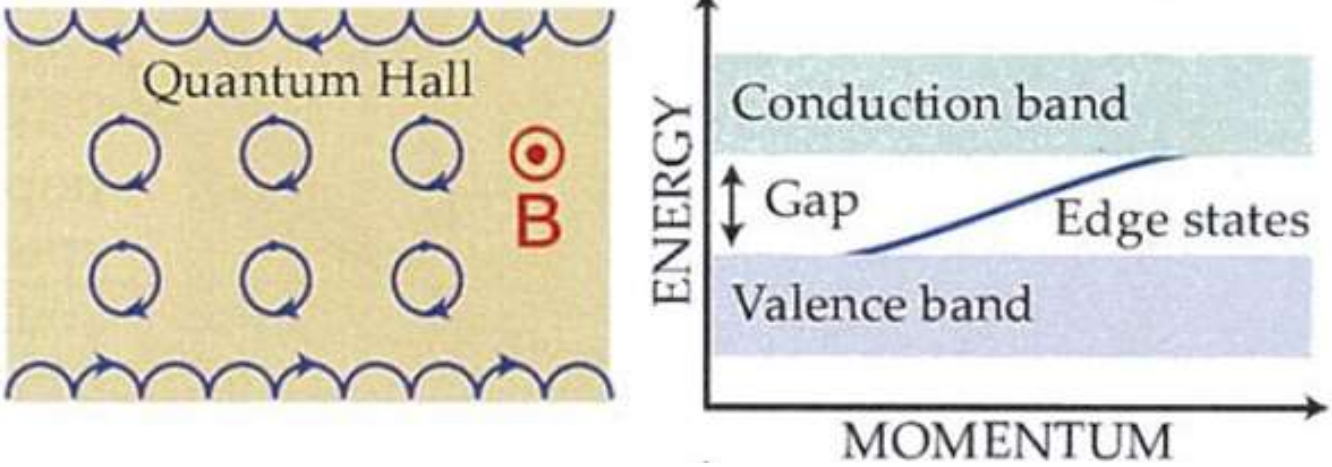

Q: High temperature IQHE without applied magnetic field?

3) Quantum anomalous Hall Effect

Model for a Quantum Hall Effect without Landau Levels: Condensed-Matter Realization of the "Parity Anomaly"

[PRL 61 (1988) 2015]

F. D. M. Haldane

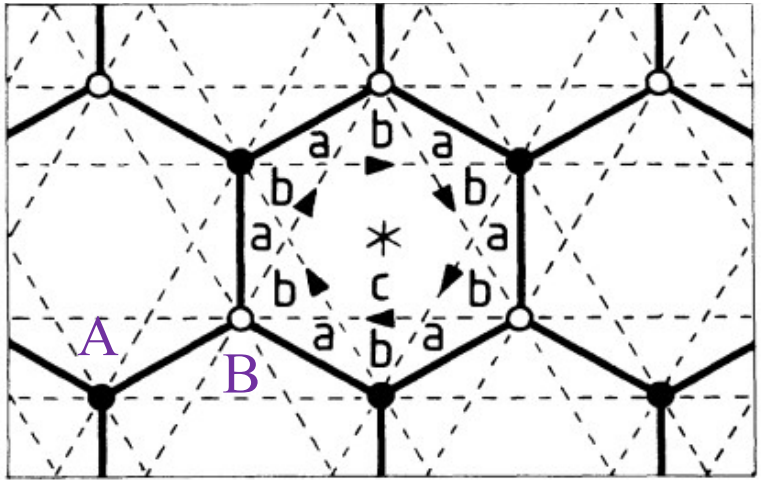

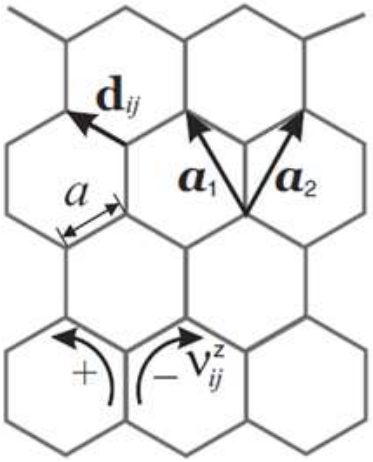

$$\nu_{ij} = \frac{\mathbf{d}_1 \times \mathbf{d}_2}{|\mathbf{d}_1 \times \mathbf{d}_2|}$$

N.B. Kane-Mele model is two copies of Haldane model with $M = 0$, $\phi = 3\pi/2$ and $\lambda_{SO} = t_2$.

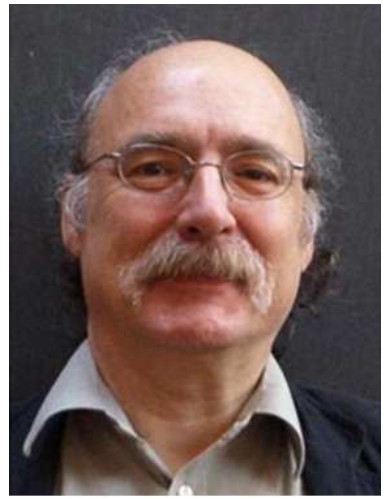

Duncan Haldane (1951 -)

Haldane's 2D honeycomb lattice model (graphene) for spinless electrons

Areas a and b are threaded by fluxes ϕ_a and $\phi_b = -\phi_a$.
Area c has no flux. $\phi = 2\pi\,(2\phi_a + \phi_b)/\phi_0$. $\varepsilon_i = \pm 1$.

$$H_H = t_1 \sum_{\langle i,j \rangle} c_i^\dagger c_j + t_2 \sum_{\langle\langle i,j \rangle\rangle} \exp(-i\nu_{ij}^z \phi) c_i^\dagger c_j + M \sum_i \varepsilon_i c_i^\dagger c_i$$

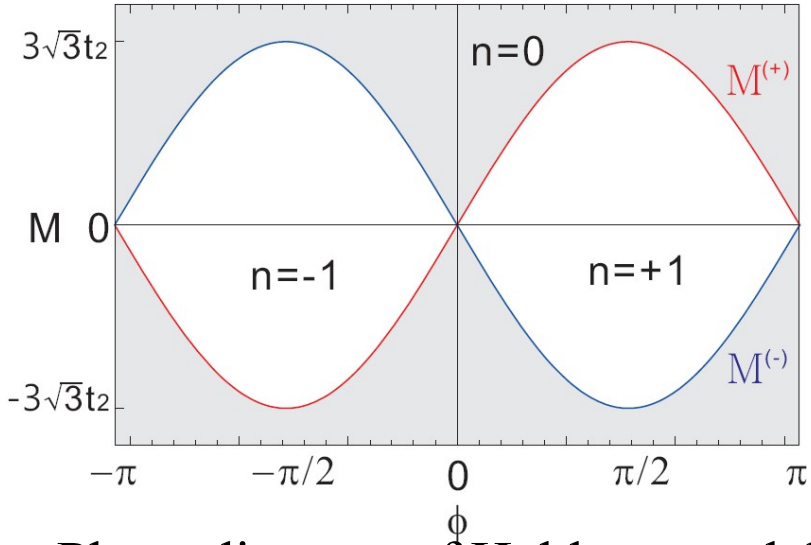

Phase diagram of Haldane model

$[|t_2/t_1| < 1/3]$

If $|M/t_2| < 3\sqrt{3}\,|\sin\phi|$,

$\sigma_{xy} = ne^2/h.$

QAHE in real systems: Magnetic impurity-doped topological insulator films

Theoretical proposal:
Bi_2Te_3, Bi_2Se_3 or Sb_2Te_3 films doped with Cr or Fe

[Yu et al., Science 329, 61 (2010)]

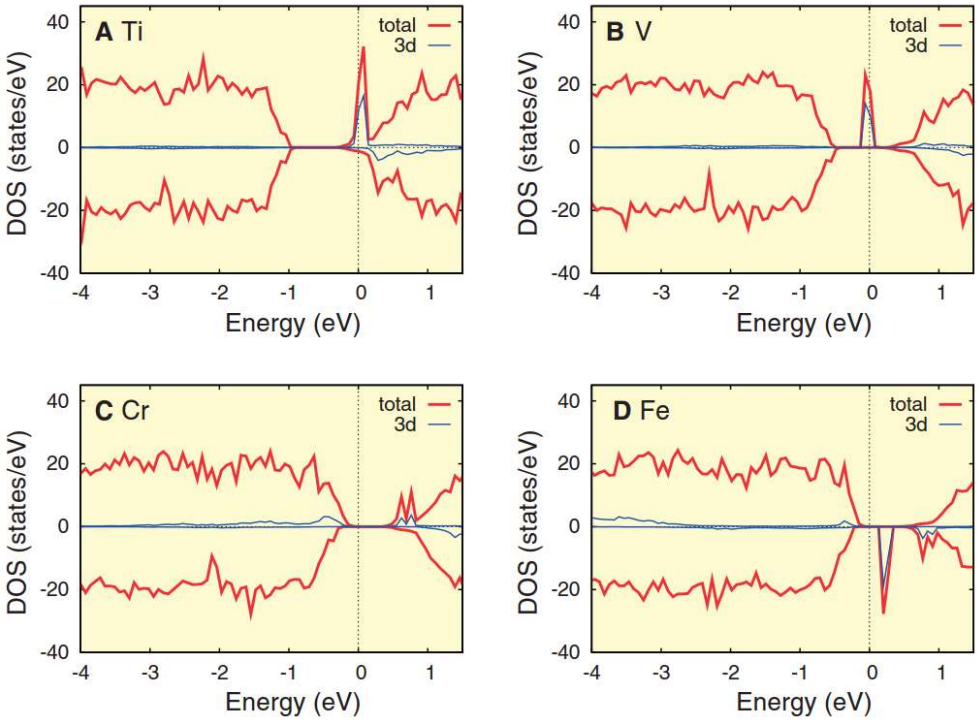

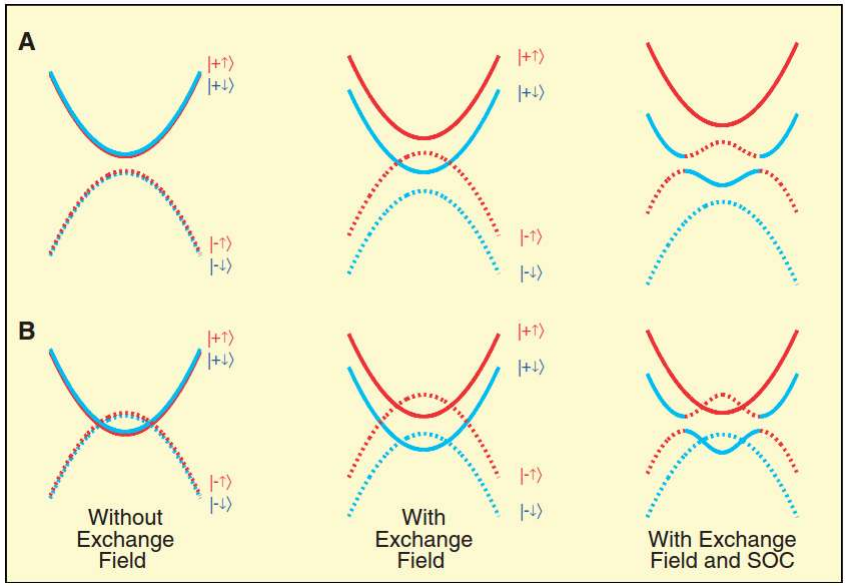

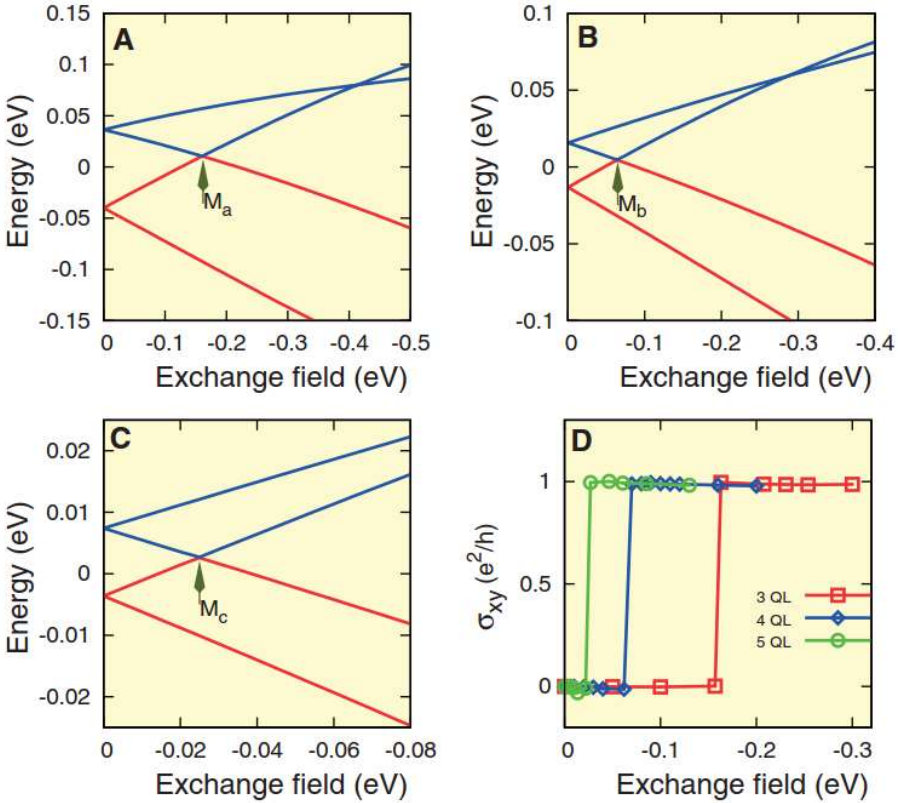

Experimental Observation of the Quantum Anomalous Hall Effect in a Magnetic Topological Insulator

Cui-Zu Chang,[1,2*] Jinsong Zhang,[1*] Xiao Feng,[1,2*] Jie Shen,[2*] Zuocheng Zhang,[1] Minghua Guo,[1] Kang Li,[2] Yunbo Ou,[2] Pang Wei,[2] Li-Li Wang,[2] Zhong-Qing Ji,[2] Yang Feng,[1] Shuaihua Ji,[1] Xi Chen,[1] Jinfeng Jia,[1] Xi Dai,[2] Zhong Fang,[2] Shou-Cheng Zhang,[3] Ke He,[2]† Yayu Wang,[1]† Li Lu,[2] Xu-Cun Ma,[2] Qi-Kun Xue[1]†

[Science 340, 167 (2013)]

First observation in $Cr_{0.15}(Bi_{0.1}Sb_{0.9})_{1.85}Te_3$ films

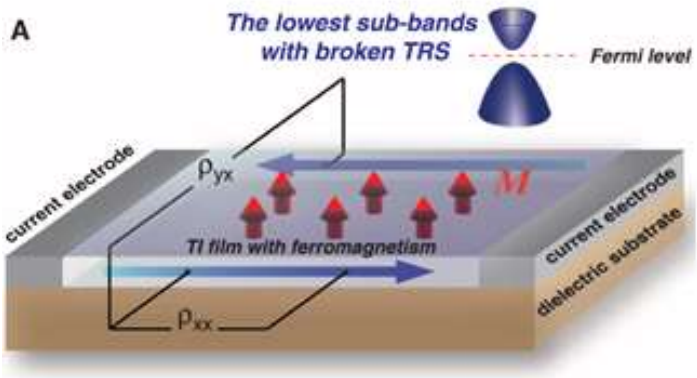

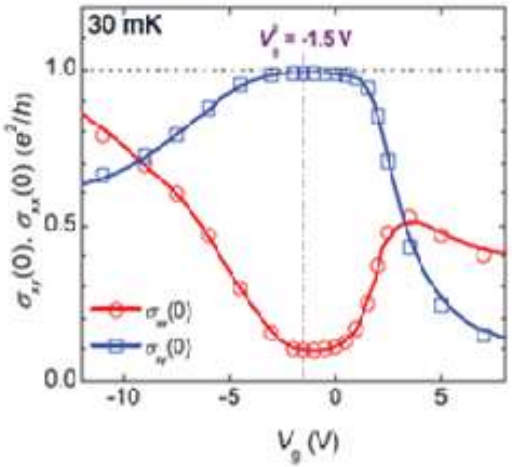

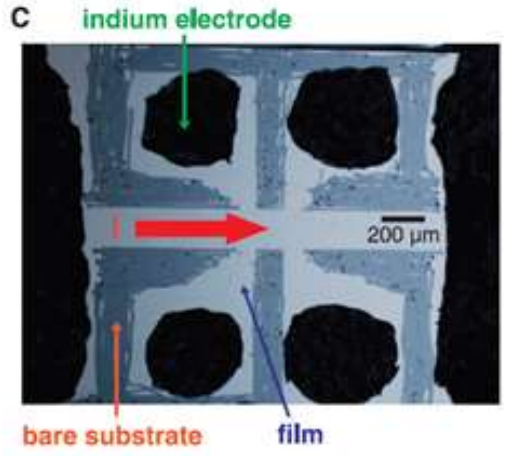

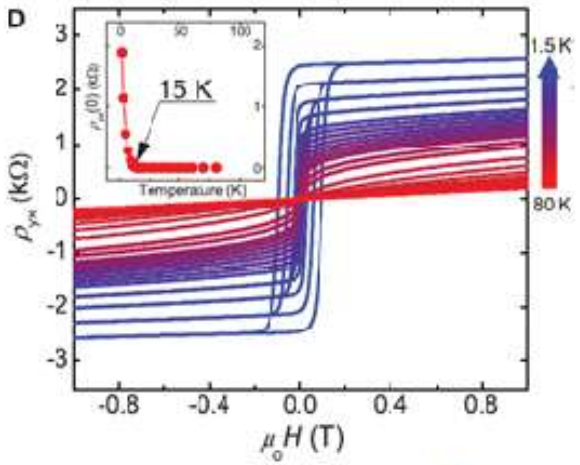

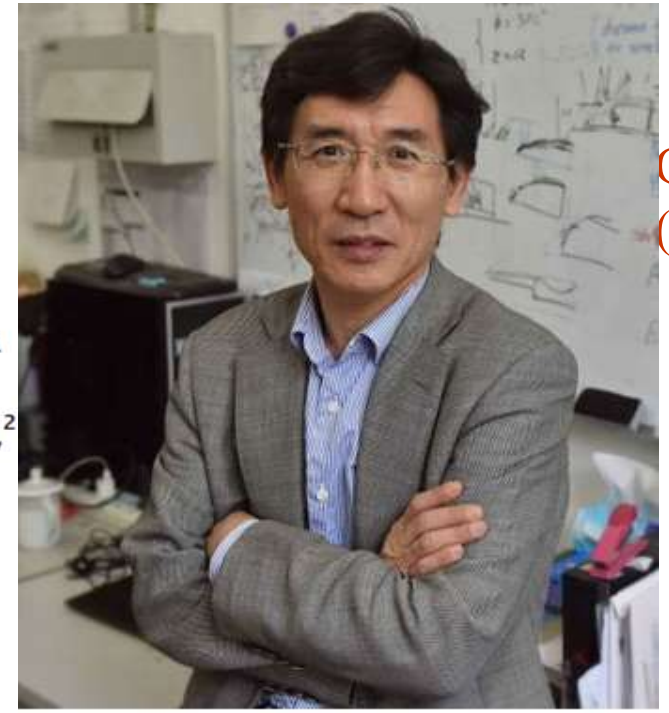

Qikun Xue (1963 -)

Xue won the 1st Future Science Prize (China, 1 M US$) for their observation of the QAHE, and superconductivity in FeSe monolayer/$SrTiO_3$.

Remaining issues:

QAHE below 30 mK due to

(a) Small band gap (~10 meV);

(b) Weak exchange coupling
T_c = ~15 K

(a) Low mobility (760 cm^2/Vs).

2. Quantum topological Hall effect in $K_{1/2}RhO_2$

1) Search for SQHE in layered 4d and 5d transition metal oxides

(a) Transition metal oxides are a fascinating family of solid state systems:
high T_c superconductivity: $YBa_2Cu_3O_{6.9}$
colossal magnetoresistance: $La_{2/3}Ca_{1/3}MnO_3$
half-metallicity for spintronics: Sr_2FeMoO_6
ferroelectricity: $BaTiO_3$
charge-orbital ordering: Fe_3O_4

(b) Layered 4d and 5d transition metal oxides as Chern insulator candidates
Electron correlations in 3d transition metal oxides are strong, which is challenging to describe, and make them become Mott (trivial) insulators.
So far, many-body theory appears unnecessary for TI research.
Layered 4d and 5d transition metal oxides have
stronger SOC (larger band gaps?),
moderate/weak correlation (easier to study?) and
intrinsic itinerant magnetism (higher mobility?).

2) Physical properties of layered oxide K_xRhO_2

(a) Crystal structure: [Shibasaki et al., JPCM 22 (2010) 115603]

Layered hexagonal γ-Na_xCoO_2-type structure ($P6_3/mmc$; No. 194) with two CdI_2-type (1T) RhO_2 layers stacked along c-axis [2f.u./cell].

(b) Interesting properties:

It is isostructural and also isoelectronic to thermoelectric and superconducting material Na_xCoO_2.

It shows significant thermopower and Seebeck coefficient, and is also expected to become superconducting at low temperatures.

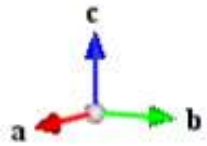

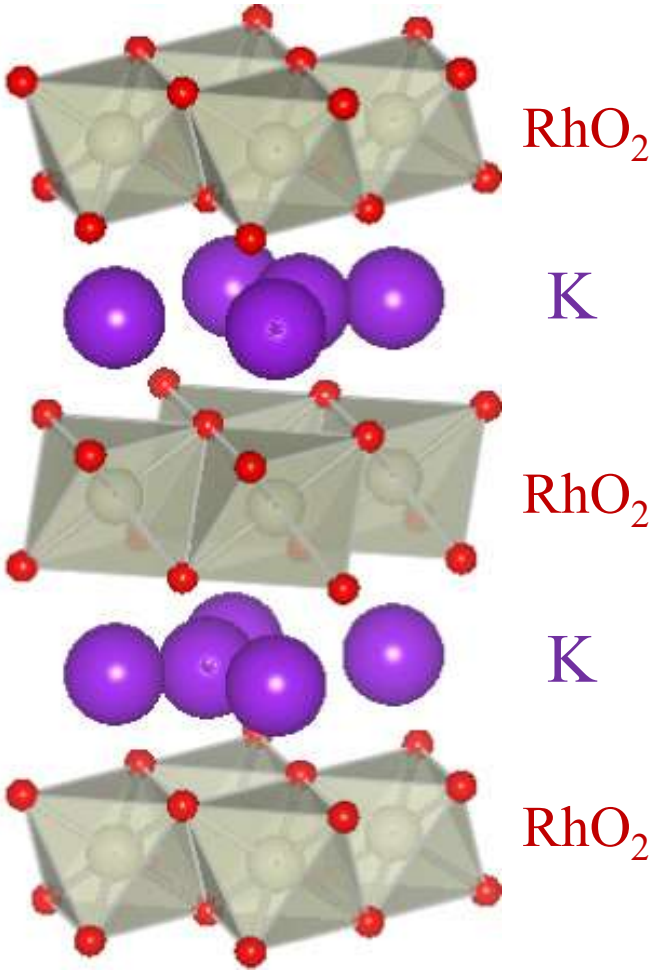

(c) Energetics of various magnetic structures in $K_{0.5}RhO_2$

[Zhou et al., PRL 116, 256601 (2016)]

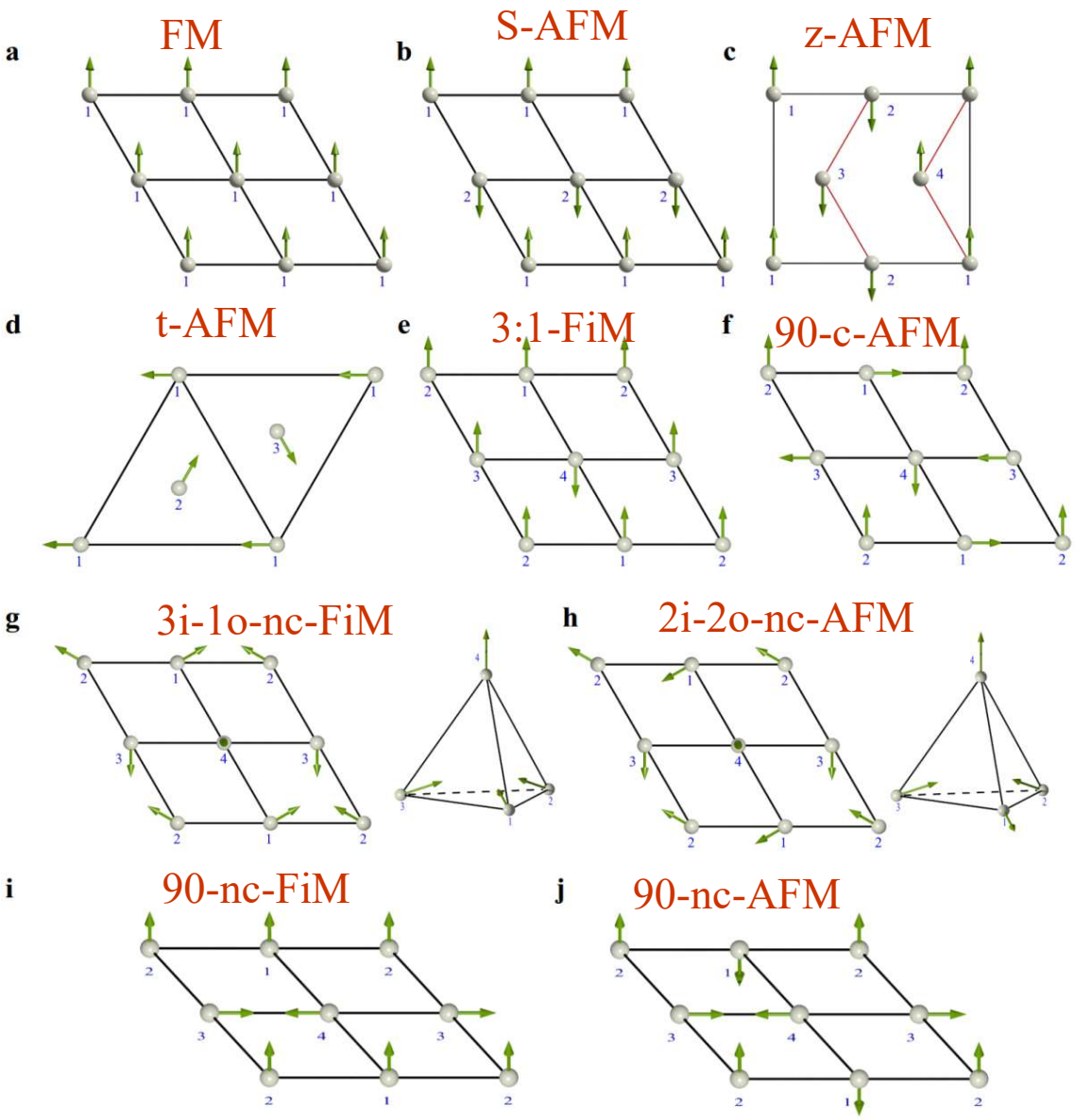

Possible metastable magnetic structures

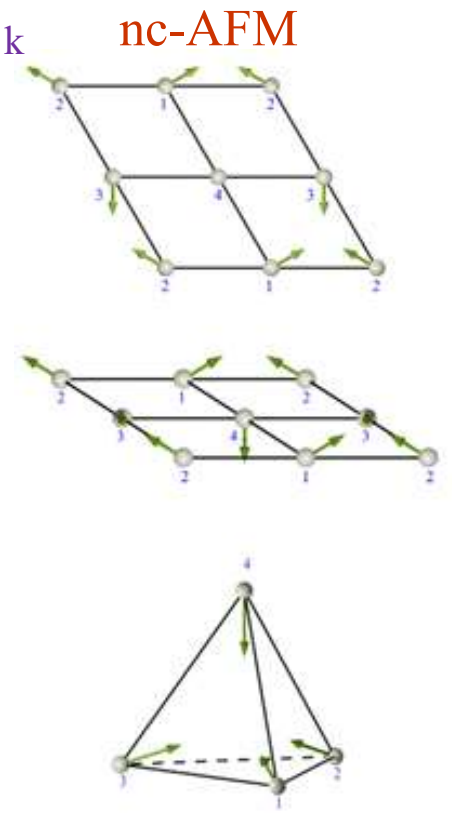

Ground state: all-in (all-out) non-coplanar antiferromagnetic structure.

Total energy (ΔE^{tot}) (meV/f.u.), total spin moment (m_s^{tot}) (μ_B/f.u.), Rh atomic spin moment (m_s^{Rh}) (μ_B/f.u.) and band gap (E_g), from GGA+U calculations. [Zhou et al., PRL 116, 256601 (2016)]

	ΔE^{tot}	m_s^{tot}	m_s^{Rh}	E_g
NM	20.19	0.00	0.00	metal
FM	2.48	0.50	0.36	metal
s-AFM	5.61	0.00	0.23	metal
z-AFM	12.85	0.00	0.23	metal
t-AFM	20.17	0.00	0.10	metal
3:1-FiM	1.99	0.00	0.06/0.15/0.24/-0.47	metal
90-c-AFM	2.20	0.00	0.23	metal
90-nc-AFM	2.14	0.00	0.23	metal
nc-AFM	0.00	0.00	0.24	0.22

Heisenberg model

$$H = E_0 - \sum_{i<j} J_{ij}\sigma_i \cdot \sigma_j$$

Exchange coupling

$J_1 = 4.4$, $J_2 = -3.6$ meV

Neel temperature $T_N = \sim 20$ K

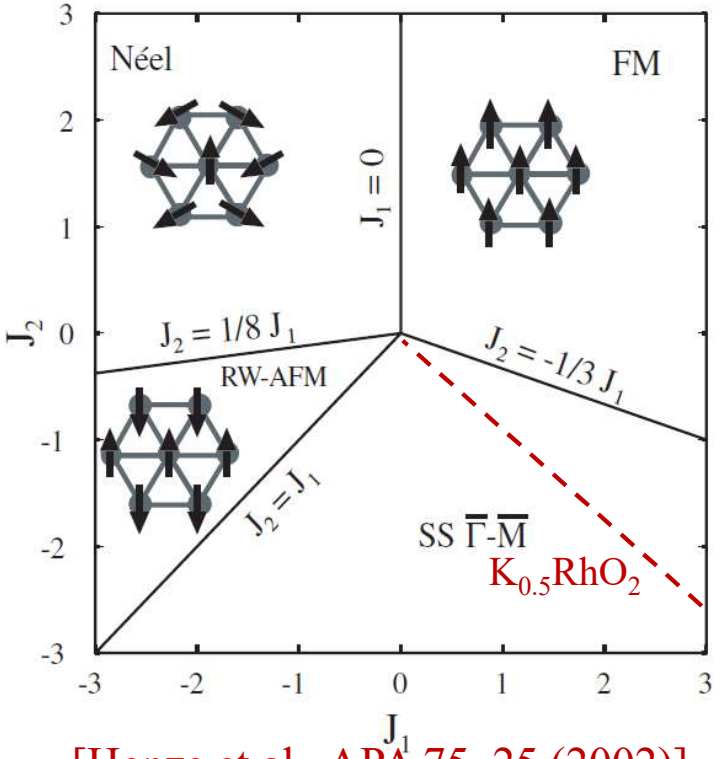

[Henze et al., APA 75, 25 (2002)]

(d) Band structure of non-coplanar antiferromagnetic structure

[Zhou et al., PRL 116, 256601 (2016)]

An insulator (E_g =0.22eV) $8(K_{1/2}RhO_2)$

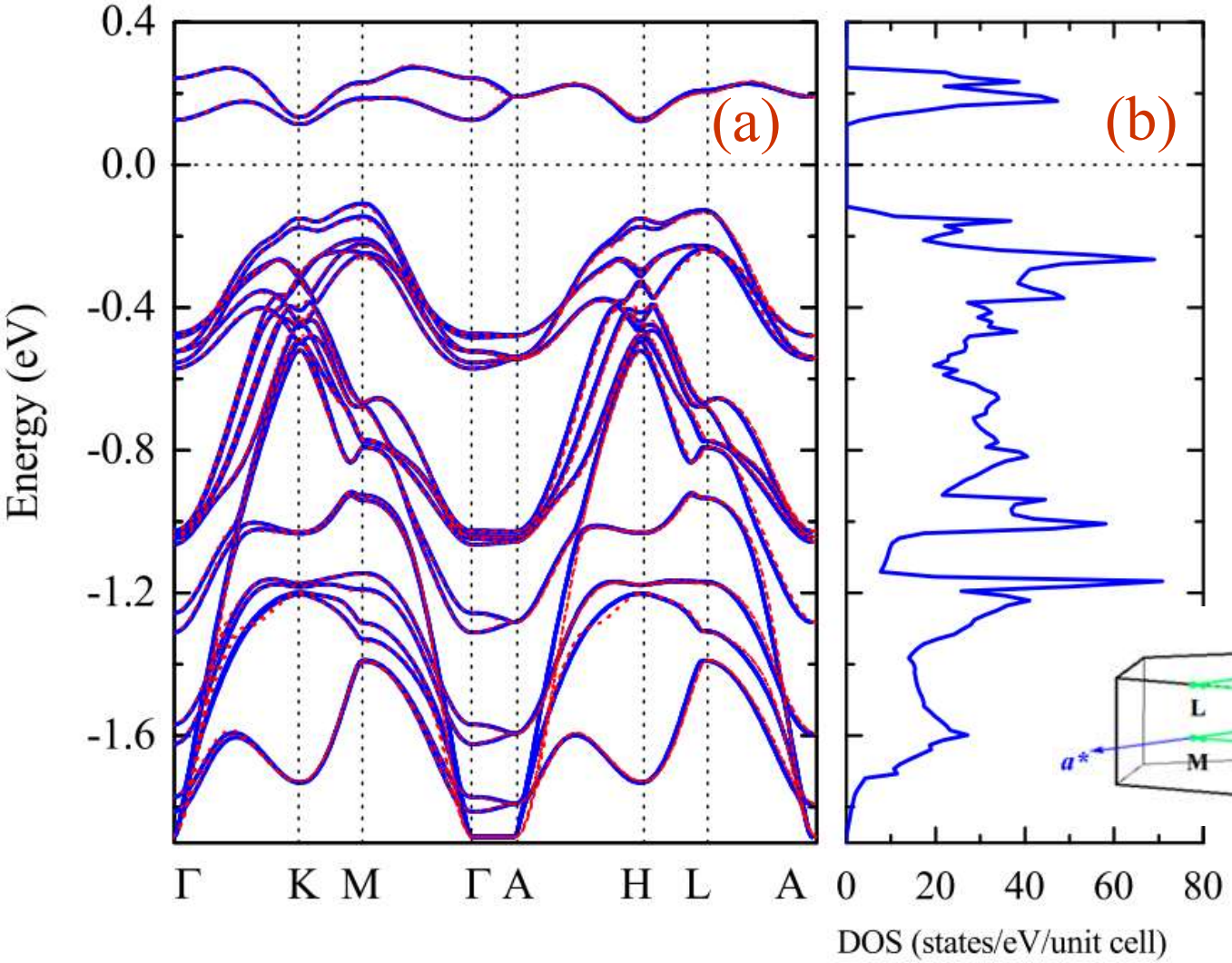

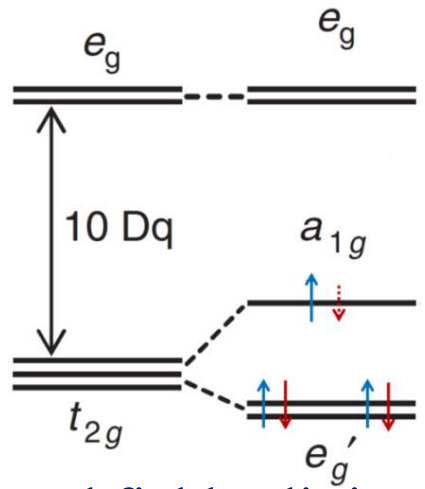

Crystal field splitting of Rh t_{2g} orbitals in $K_{1/2}RhO_2$ with Rh a_{1g} is ¾ filled.

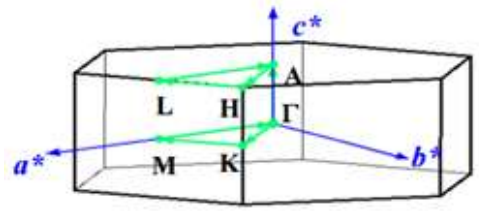

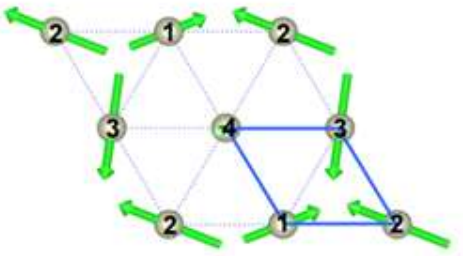

In (a), blue solid lines from GGA+U and red dotted lines from MLWFs interpolations.

Is it a topologically trivial or nontrivial insulator?

(e) Unconventional quantum anomalous Hall phase

A Chern insulator

Anomalous Hall conductivity

$$\sigma_{AH} = -\frac{e^2}{\hbar(2\pi)^3}\int d^3k \sum_n f(\varepsilon_n(\mathbf{k}))\Omega_n^z(\mathbf{k})$$

$$\Omega_n^z(\mathbf{k}) = -\sum_{n'\neq n} \frac{2\,\mathrm{Im}\langle \mathbf{k}n | v_x | \mathbf{k}n'\rangle\langle \mathbf{k}n' | v_y | \mathbf{k}n\rangle}{(\omega_{\mathbf{k}n} - \omega_{\mathbf{k}n'})^2}$$

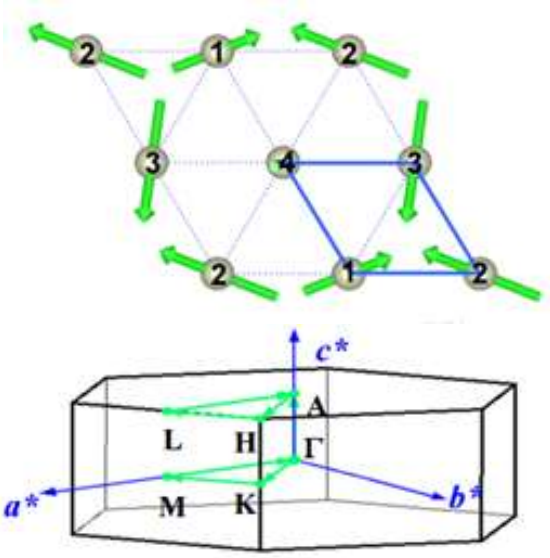

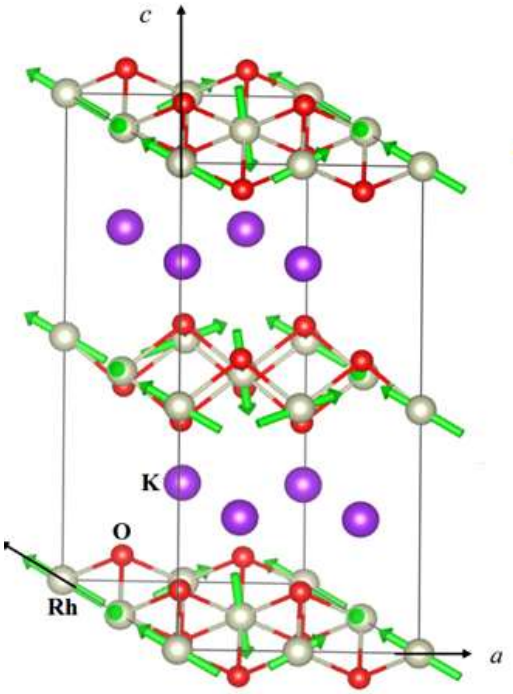

For a 3D Chern insulator,

$$\sigma_{AH} = n_c \frac{e^2}{hc}$$

n_c is an integer (Chern number)

Thus, nc-AFM state is a QAH phase with $n_c = 2$.

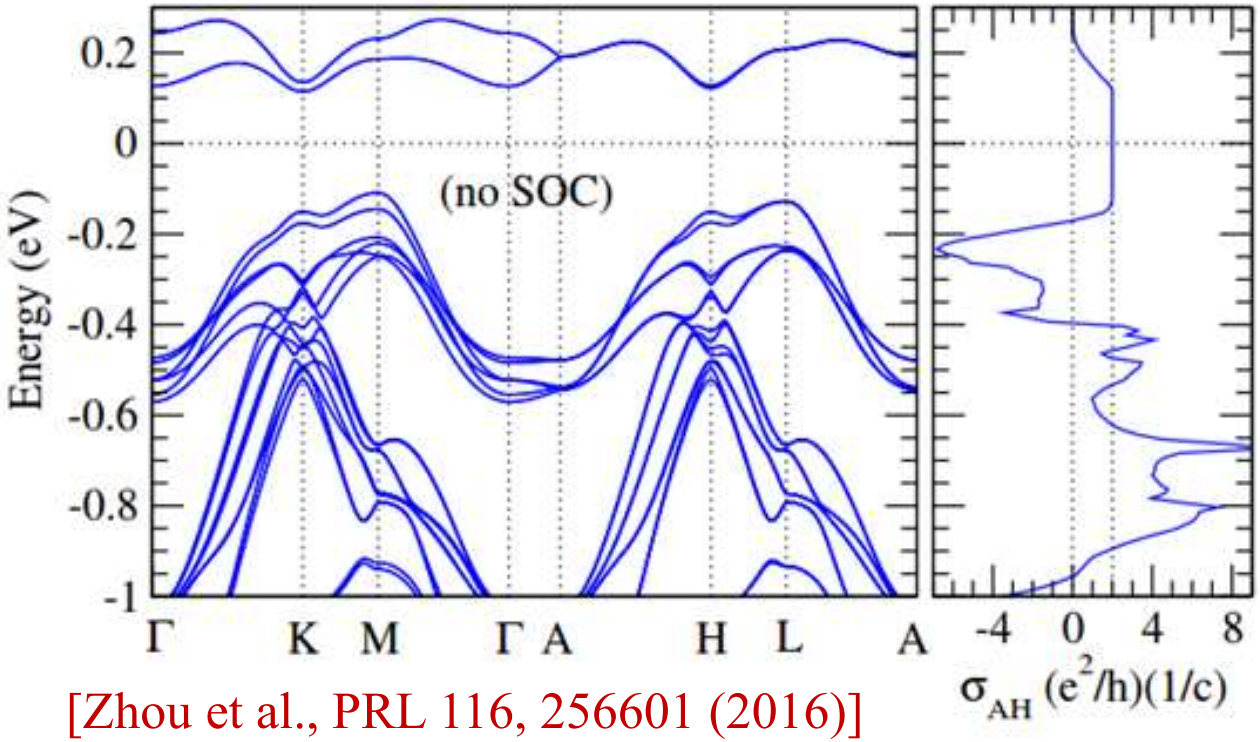

[Zhou et al., PRL 116, 256601 (2016)]

(f) Nature of the quantum anomalous Hall phase

Spin chirality, Berry phase and topological Hall effect

[Taguchi et al., Science 291, 2573 (2001)]

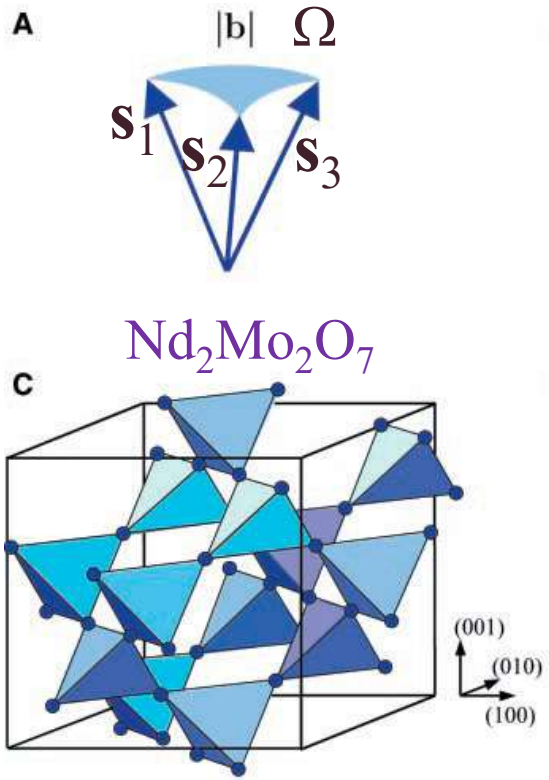

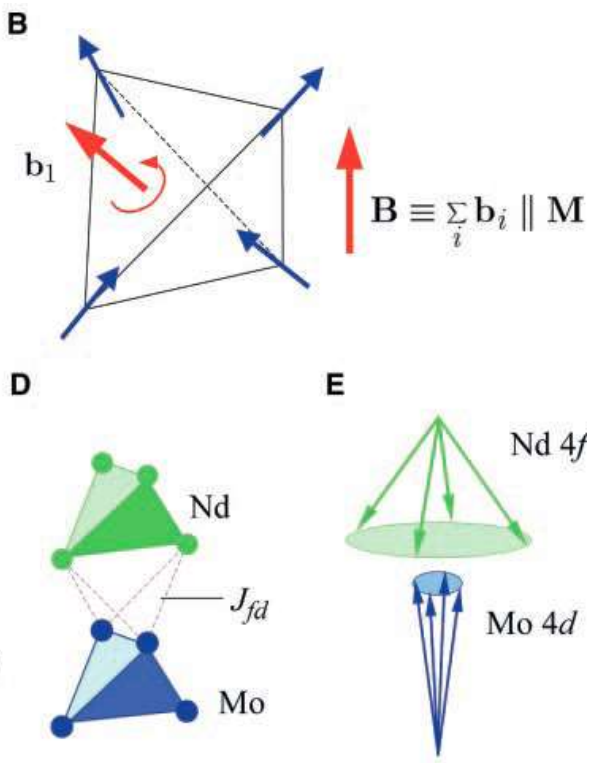

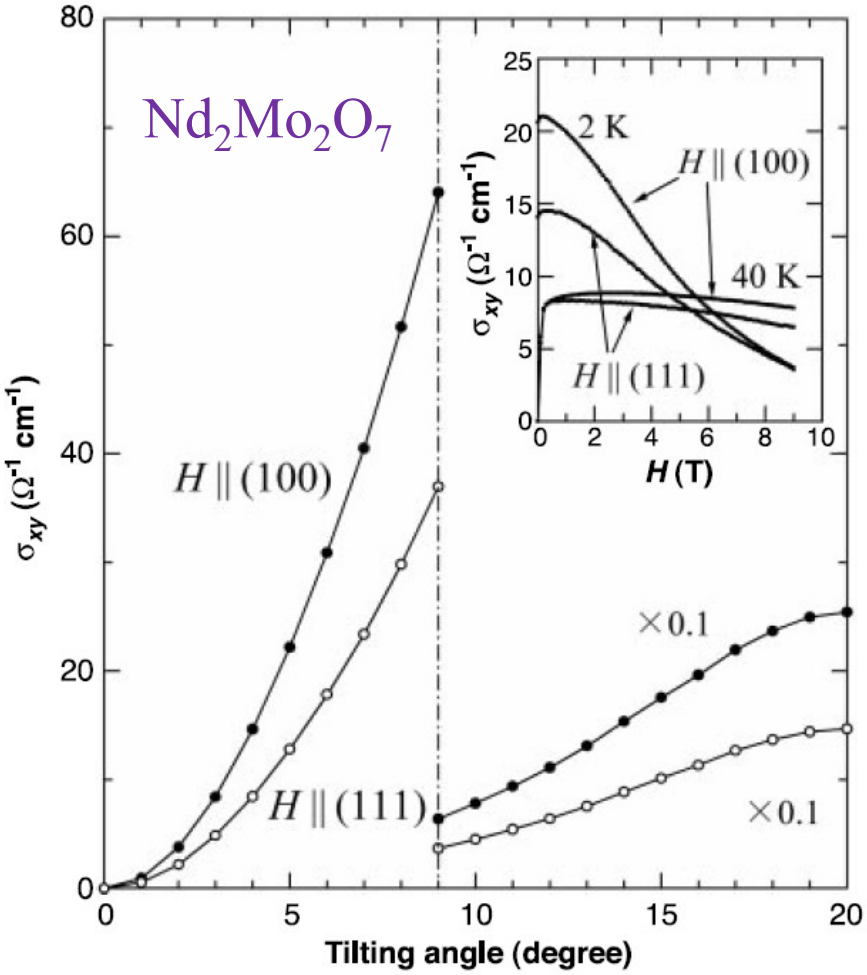

Spin chirality

$$\kappa = \sum_{i,j,k} \mathbf{s}_i \cdot (\mathbf{s}_j \times \mathbf{s}_k).$$

solid angle Ω,

Berry phase $\gamma = \Omega / 2$

Topological Hall effect: Anomalous Hall effect purely due to Berry phase produced by spin-chiraty in the noncoplanar magnetic strucure.

[Zhou et al., PRL 116, 256601 (2016)]

A conventional QAH phase is caused by the presence of FM and SOC!

Here, $m_s^{tot} = 0$ and no SOC; thus QAH phase is unconventional.

AHC is due to nonzero scalar spin chirality in nc-AFM structure,

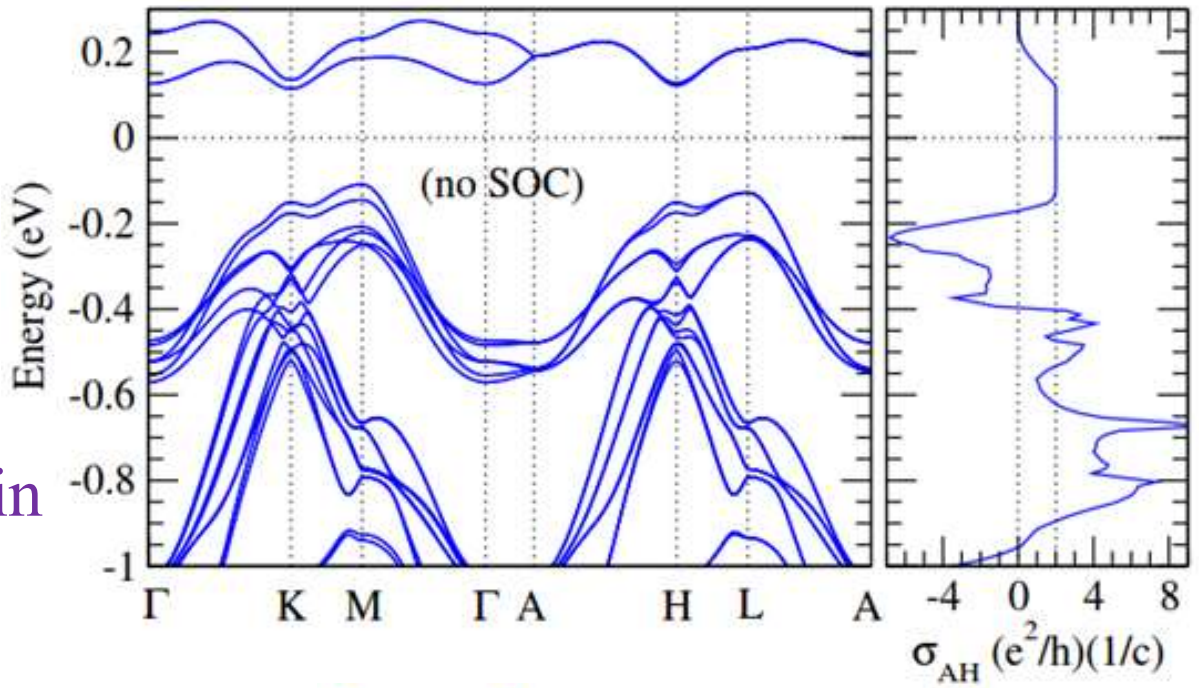

Total solid angle $\Omega = 4\pi$,

Berry phase $\gamma = \Omega / 2$,

Chern number $n_c = (\gamma / 2\pi) \times 2 = 2$,

AHC $\sigma_{AH} = 2e^2/h$.

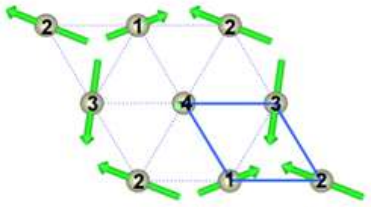

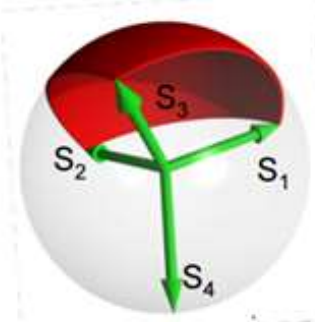

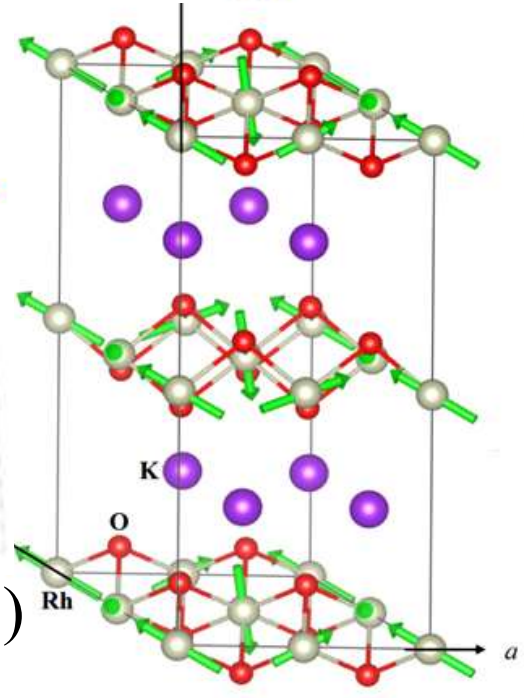

So it is the exotic quantum topological Hall effect due to the topologically nontrivial chiral magnetic structure!

$$\kappa = \sum_{i,j,k} \mathbf{s}_i \cdot (\mathbf{s}_j \times \mathbf{s}_k)$$

V. Conclusions and outlook

Quantum-mechanics-based first-principles calculations have become a powerful tool in condensed matter and materials physics research, thanks to advanced theories, numerical algorithms and modern computers.

In particular, they (1) prove crucial to understand intriguing phenomena occurring in condensed matter systems, (2) enable us to uncover/predict new materials with exotic properties and (3) allow us to design functional materials with desired properties for technological applications.

Analytically solvable quantum problems are very limited. On the other hand, new computing paradigms such as quantum computing are emerging on the horizon. Thus, first-principles calculations will play an increasingly important role in condensed matter and material physics research.

Acknowledgements:

Discussion and Collaborations:

Horng-Tay Jeng (NTHU), Di-Jing Huang + his team (NSRRC)
Qian Niu (UT Austin), Tsung-Wei Chen (NTU->NSYSU)
Shuichi Murakami (Tokyo Inst. Techno.)
Naoto Nagaosa (Tokyo U.)
Bo Gu, Sadamichi Maekawa (JAEA)
Jian Zhou and his team (Nanjing U.)
Qi-Feng Liang (Shaoxing U.)

Supports:

Ministry of Science and Technology, Academia Sinica,
National Center for Theoretical Sciences, Kenda Foundation

Also thank you for your attention!